Primary and secondary biomass burning aerosols determined by proton nuclear magnetic resonance (^{1}H-NMR) spectroscopy during the 2008 EUCAARI campaign in the Po Valley (Italy).

M. Paglione[1], S. Saarikoski[2], S. Carbone[2], R. Hillamo[2], M. C. Facchini[1], E. Finessi[1], L. Giulianelli[1], C. Carbone[1], S. Fuzzi[1], F. Moretti[3], E. Tagliavini[3], E. Swietlicki[4], K. Eriksson Stenström[4], A. S. H. Prevot[5], P. Massoli[6], M. Canaragatna[6], D. Worsnop[6], S. Decesari[1].

[1] *National Research Council (CNR), Institute of Atmospheric Sciences and Climate (ISAC), Bologna, Italy (m.paglione@isac.cnr.it, +39-051-6399578);*

[2] Finnish Meteorological Institute, Air Quality, Helsinki, Finland;

[3] *Centro Interdipartimentale di Ricerca per le Scienze Ambientali (CIRSA), University of Bologna, Ravenna, Italy;*

[4] Lund University, Department of Physics, Lund, Sweden;

[5] Paul Scherrer Institute (PSI), Laboratory of Atmospheric Chemistry, Villigen, Switzerland;

[6] Aerodyne Research, Inc. Billerica, MA, USA.

Abstract

Atmospheric organic aerosols are generally classified into primary and secondary (POA and SOA) according to their formation processes. An actual separation, however, is challenging when the timescales of emission and of gas-to-particle formation overlap. The presence of SOA formation in biomass burning plumes leads to scientific questions about whether the oxidized fraction of biomass burning aerosol is rather of secondary or primary origin, as some studies would suggest, and about the chemical compositions of oxidized biomass burning POA and SOA. In this study, we apply nuclear magnetic resonance (NMR) spectroscopy to investigate the functional group composition of fresh and aged biomass burning aerosols during an intensive field campaign in the Po Valley, Italy. The campaign was part of the EUCAARI project and was held at the rural station of San Pietro Capofiume in spring 2008. Factor analysis applied to the set of NMR spectra was used to apportion the wood burning contribution and other organic carbon (OC) source contributions, including aliphatic amines. Our NMR results, referred to the polar, water-soluble fraction of OC, show that fresh wood burning particles are composed of polyols and aromatic compounds, with a sharp resemblance with wood burning POA produced in wood stoves, while aged samples are clearly

34 depleted of alcohols and are enriched in aliphatic acids with a smaller contribution of aromatic

35 compounds. The comparison with biomass burning organic aerosols (BBOA) determined by high

36 resolution aerosol mass spectrometry (HR-TOF-AMS) at the site shows only a partial overlap

37 between NMR BB-POA and AMS BBOA, which can be explained by either the inability of BBOA

38 to capture all BB-POA composition, especially the alcohol fraction, or the fact that BBOA account

39 for insoluble organic compounds unmeasured by the NMR. Therefore, an unambiguous

40 composition for biomass burning POA could not be derived from this study, with NMR analysis

41 indicating a higher O/C ratio compared to that measured for AMS BBOA. The comparison between

42 the two techniques substantially improves when adding factors tracing possible contributions from

43 biomass burning SOA, showing that the operational definitions of biomass burning organic aerosols

44 are more consistent between techniques when including more factors tracing chemical classes over

45 a range of oxidation levels. Overall, the non-fossil total carbon fraction was 50 % - 57 %, depending

46 on the assumptions on the ^{14}C content of non-fossil carbon, and the fraction of organic carbon

47 estimated to be oxidized organic aerosol (OOA) from HR-TOF-AMS measurements was 73% -

48 100% modern.

49

50 **1. Introduction**

51 The adoption of new regulatory actions for reducing the emissions from fossil fuel combustion have

52 certainly contributed to measurable decreases in atmospheric particulate matter concentrations in

53 several areas in North America and Europe in the last two decades (Barmpadimos et al., 2011,

54 2012; Hand et al. 2012). This decreasing trend was flatter during the 2000s compared to the 1990s

55 in spite of the fact that emissions of sulphur, nitrogen and carbonaceous compounds from fossil fuel

56 combustion have decreased steadily in Europe throughout the whole period (Harrison et al., 2008).

57 Clearly, sulphate aerosols, whose reduction certainly boosted the PM10 reduction in Europe during

58 the 1990s, are nowadays of secondary importance with respect to other aerosol components such as

59 ammonium nitrate and organic aerosol (OA), which are becoming new targets. The evaluation of

60 abatement strategies for the organic fraction of particulate matter is particularly challenging due to

61 the number of anthropogenic and natural sources contributing to OA and to the complexity of the

62 atmospheric processes controlling the concentrations of organic compounds susceptible to partition

63 from the gas to the aerosol phase. There is actually no consensus on the best source apportionment

64 method for particulate organic carbon (OC) and no single method would suffice, although important

65 scientific achievements about its origin and atmospheric processing have been obtained in the last

66 years. Some recent findings, relevant for the present study, are: a) the fact that a large fraction of

67 modern carbon is found in OC even in environments highly impacted by fossil-fuel combustion

68　(Hodzic et al. 2010); b) the importance of residential biofuel combustion emissions worldwide,

69　including industrialized countries (Bond et al., 2004; Kulmala et al., 2011); c) the fact that the

70　budget of the OC emitted by combustion sources often includes a non-negligible fraction of

71　secondary origin, i.e., forming in the plume by secondary reactions (Robinson et al. 2007; Nordin et

72　al., 2013). These findings suggest that the presence of primary and secondary organic aerosol

73　(respectively "POA" and "SOA") from biomass burning is much more significant than believed in

74　the past, and perhaps up to 30% of the global aerosol OC budget (Hallquist et al., 2009).

75　In this study, we investigate the contribution of primary and secondary biomass burning to

76　oxygenated organic aerosols in the rural Po Valley, Italy, in early spring: a period of the year during

77　which diffuse wood burning from domestic heating systems is still active in the valley, and the

78　meterorological conditions often favour stagnation of pollutants. In a previous paper (Saarikoski et

79　al., 2012) we showed that under stable meteorological conditions the diurnal change in atmospheric

80　stratification following the development of the planetary boundary layer was responsible for drastic

81　changes in submicron aerosol composition, with fresh particulates rich in semivolatile compounds

82　during the night and early morning, and more aged particles occurring in the middle of the day and

83　in the afternoon. Atmospheric concentrations of particulate organic matter including fractions

84　apportioned to biomass burning sources could be determined owing to the employment of an

85　Aerodyne high-resolution time-of-flight mass spectrometer (HR-TOF-AMS, hereafter AMS) (De

86　Carlo et al., 2006) and Positive Matrix Factorization (PMF) analysis (Ulbrich et al., 2009). PMF

87　analysis of AMS datasets provides factors for organic aerosol sources and corresponding

88　contributions to OC concentrations. PMF is becoming common for organic source apportionment

89　(Zhang et al., 2005; Lanz et al., 2007) and factor analysis of AMS data using PMF in its diverse

90　implementations (including e.g. ME-2) has extracted biomass burning organic aerosol (BBOA)

91　factors in multiple sites (Aiken et al., 2010; Elsasser et al., 2012; Crippa et al., 2013a etc.).

92　Generally, the BBOA factors appear to reflect directly emitted primary biomass burning aerosol (p-

93　BBOA), but the degree to which p-BBOA and secondary organic aerosol formed from biomass

94　burning emissions are separated in PMF analyses have not been extensively examined.

95　Here we use ancillary information from tracer compounds, some of which are already included in

96　the study of Saarikoski et al. (2012), and other spectroscopic techniques suitable for organic source

97　attribution, presented here for the first time, such as nuclear magnetic resonance (NMR)

98　spectroscopies (Hallquist et al., 2009) to investigate the separation of primary and secondary

99　biomass burning related emissions during the Po Valley Spring measurements. Proton NMR (^{1}H-

100　NMR) spectroscopy in particular has been already successfully used to characterise biomass

101　burning aerosols in tropical environments (Decesari et al., 2006), and has also been proposed as a

tool for source attribution of water-soluble organic aerosol including biomass burning particles (Decesari et al., 2007). In this paper, we compare the spectral fingerprints of wood burning aerosol as determined by HR-TOF-AMS and ^{1}H-NMR spectroscopies during the 2008 EUCAARI experiment in the Po Valley, and we interpret the chemical composition of NMR-determined biomass burning aerosol on the basis of laboratory and field data obtained in past and parallel experiments.

2 Experimental

2.1 The EUCAARI 2008 Po Valley campaign.

The measurements were conducted at the San Pietro Capofiume (SPC) measurement station "G. Fea" (44°39'0'' N, 11°37'0'' E; Decesari et al., 2001) from 30 March to 20 April 2008. The station is located about 30 km northeast from the city of Bologna in an area of the Po Valley open to Adriatic Sea to the east side, but surrounded by densely populated areas on its southern, western and northern sides. The station of San Pietro Capofiume belongs to the network ARPA-ER ("Agenzia Regionale Prevenzione e Ambiente – Emilia-Romagna") for meteorological observations and air quality monitoring. The station regularly hosts measurements of aerosol chemical and physical measurements and of aerosol optical properties and light extinction run by ISAC-CNR, ARPA-ER and the University of Eastern Finland. During the 2008 EUCAARI experiment, a suite of additional aerosol measurements were implemented including AMS (Saarikoski et al., 2012), HTDMA and air ion spectrometers (Manninen et al., 2010).

On the basis of the meteorological conditions and back-trajectory analysis, five periods can be distinguished: Period I (30 March – 6 April) characterized by vertical atmospheric stability, relatively low wind speeds (2.4 m/s on average), high pollution levels and marked diurnal variations in aerosol concentration and composition; Period II (7 April) with low concentrations and significant transport from outside the Valley suggested also by the highest mean wind speed of the campaign (4.3 m/s on average); Period III (8 to 11 April) with re-established stable conditions, lower wind speed (1.9 m/s on average), high pollution levels, high humidity, little diurnal variations and transport of maritime air masses; Period IV (April 11 and 12) characterized by atmospheric instability, again higher wind speed (3.2 m/s on average) and very low aerosol concentrations; Period V (April 12 to 20) with high variability (with wind speeds ranging between 0.2 and 6.9 m/s), intermittent precipitation events and moderate average pollutant concentrations. The PM1 chemical composition observed during the five periods reflected the different meteorological and atmospheric transport conditions, with higher concentrations of ammonium nitrate during the polluted days and

135 greater proportions of ammonium sulphate in background conditions (Saarikoski et al., 2012), in
136 line with a behaviour typical of many continental environments.

137

2.2. Sampling and off-line chemical analysis

139 A dichotomous sampler (Universal Air Sampler, model 310, MSP Corporation) at a constant
140 nominal flow of 300 l/min was employed from 1st to 14th of April 2008 to collect fine particles with
141 ambient diameter < 1 μm on pre-washed and pre-baked quartz-fiber filters (Whatman, Ø = 9 cm).
142 Typically, two filters were sampled every day: a "daytime" (D) PM_1 sample was collected from
143 ~10:00 to ~17:00 (local time, UTC+2) followed by an "evening/night-time" (N) sample collected
144 from ~18:00 to ~09:00. Exceptionally, long-time integrated samples (n = 3, lasting 32, 24 and 24
145 hours) were taken using an Andersen PM10 high-volume (HiVol) sampler at critical flow (1.13 m^3
146 min^{-1}) equipped with quartz-fiber filters (Whatman, 8×10 in.). All samples were stored frozen until
147 chemical analysis.

148 Total Carbon (TC) content was measured directly from small sub-samples of the quartz-fiber filters
149 (1 cm^2) by evolved gas analysis. Measurements were performed by a Multi N/C 2100 analyser
150 (Analytik Jena, Germany) equipped with a module for solid samples. Samples were oxidized in an
151 atmosphere of pure oxygen and by applying a temperature ramp (up to 950°C). TC was measured as
152 total evolved CO_2 by a non-dispersive infrared (NDIR) analyser (Gelencser et al., 2000).

153 The remaining portion of each filter was extracted with deionized ultra-pure water (Milli-Q) in an
154 ultrasonic bath for 1 h and the water extract was filtered on PTFE membranes (pore size: 0.45 μm)
155 in order to remove suspended particles. Aliquots of the water extracts were used to determine the
156 water-soluble organic carbon (WSOC) content by a Multi N/C 2100 total organic carbon analyser
157 (Analytik Jena, Germany) using the interface for liquid sample injection. The analysis provided the
158 WSOC concentration in the extracts upon correction for the inorganic carbon (carbonate)
159 concentration (Rinaldi et al., 2007). The difference between TC and WSOC and carbonate carbon
160 resulted in the water-insoluble carbon (WINC), which accounts for insoluble organic compounds +
161 elemental carbon.

162 Concentrations of major inorganic ions (NH_4^+, Na^+, K^+, Ca^{2+}, Mg^{2+}, Cl^-, NO_3^-, SO_4^{2-}) and some
163 organic acids (i.e., oxalate) were determined in the water extracts of the PM1 filters by ion
164 chromatography (IC) using the same protocol adopted for the Berner impactor samples analyzed in
165 the same experiment (Saarikoski et al., 2012).

166 The remaining aliquots of the water extracts were dried under vacuum and re-dissolved in
167 deuterium oxide (D_2O) for functional group characterization by proton-Nuclear Magnetic
168 Resonance (^{1}H-NMR) spectroscopy (Decesari et al., 2000). The extracts of the seven samples

169 collected during Periods IV and V of the campaign were lumped into three samples to increase
170 sample load and sensitivity of the analysis. The ^{1}H-NMR spectra were acquired at 400 MHz with a
171 Varian Mercury 400 spectrometer in a 5mm probe. Sodium 3-trimethylsilyl-(2,2,3,3-d4) propionate
172 (TSP-d4) was used as referred internal standard, adding 50 μl of a TSP-d4 0.05% (by weight)
173 solution in D_2O (1.5 μmolH belonging to the standard in the probe). ^{1}H-NMR spectroscopy in
174 protic solvents provides the speciation of hydrogen atoms bound to carbon atoms. On the basis of
175 the range of frequency shifts (the chemical shift, ppm) in which the signals occur, they can be
176 attributed to different H-C-containing functional groups. Detection limits for an average sampling
177 volume of 500 m^3 were of the order of 3 nmol m^{-3} for each functional group.

178 Since aliphatic carbonyls or carboxylic groups don't have detectable protons, their concentrations
179 can be detected by proton NMR spectroscopy only indirectly, on the basis of the intensity of
180 resonances between 1.9 – 3.0 ppm of chemical shift, which can be attributed to aliphatic groups
181 adjacent to an unsaturated carbon atom, e.g., HC-C=O, HC-COOH or HC-C=C. Since aromatic and
182 vinyl groups are relatively scarce in WSOC atmospheric samples, the unsaturated oxygenated
183 groups provide the greatest contribution. The approach of Decesari et al. (2007) includes a
184 correction for the contribution of benzylic groups (CH-Ar), which is assumed to be proportional to
185 the total aromatic protons and it is subtracted from total H-C-C= moieties to derive the aliphatic
186 groups containing oxygenated unsaturated groups (i.e. carbonyls and carboxyls), HC-C=O.

187 Recent works (Tagliavini et al. 2006; Moretti et al. 2008) introduced a methodology for direct
188 determination of carbonyls and carboxylic groups by coupling chemical derivatization to proton
189 NMR spectroscopy, and was applied to the present study. Briefly, carboxylic acids were converted
190 to methyl-esters by reaction with diazomethane and the concentration of the products was
191 quantified by integrating the band between 3 and 4 ppm in the ^{1}H-NMR spectrum after subtraction
192 of the signals of the underivatized sample. An analogous procedure was applied for carbonyls,
193 which were derivatized to methyloximes by reaction with O-methyl-hydroxylamine. A detailed
194 discussion of the methodology is presented in Moretti et al. (2008). The chemical derivatization
195 procedure is labour intensive and, in its current version, it is not designed for the analysis of large
196 number of samples. In this study it was employed at an explorative level mainly to probe the
197 oxygenated functional group distribution information. The advantages of chemical derivatization –
198 NMR analysis as a benchmark methodology for fast AMS measurement are the specificity of
199 functional group derivatization and the "soft", non-destructive NMR detection.

200 An anion-exchange high performance liquid chromatography (HPLC-TOC) technique, already
201 described by Mancinelli et al. (2007) was also employed on one aerosol sample collected during the
202 EUCAARI field campaign. The technique, based on a purely inorganic buffer, allows to fractionate

6

203 WSOC into four chemical classes, namely neutral/basic compounds (NB), mono-acids (MA), di-

204 acids (DA) and poly-acids (PA, representative of humic-like substances), and to quantify them by

205 off-line TOC analysis. The same Multi N/C 2100 total organic carbon analyzer used for total

206 WSOC analysis was also employed for analysis of the chromatographic fractions.

207

2.3 Factor analysis of NMR spectra

209 Factor analysis (FA), in the broad sense, includes several multivariate statistical techniques that

210 have been extensively used in the last years in atmospheric sciences for aerosol source

211 apportionment on the basis of the internal correlations of observations at a receptor site, or receptor

212 modelling (Viana et al., 2008). Regardless of the specific constraints imposed and of the different

213 algorithms, all the different methods of FA are based on the same bilinear model that can be

214 described by equation (1):

$$x_{ij} = \sum_{k=1}^{p} g_{ik} f_{kj} + e_{ij}$$

215 **(1)**

216 where x_{ij} refers to a particular experimental measurement of concentration of species *j* (one of the

217 analytes or, here, one point of the mass or NMR spectrum) in one particular sample *i*. Individual

218 experimental measurements are decomposed into the sum of *p* contributions or sources, each one of

219 which is described by the product of two elements, one (f_{kj}) defining the relative amount of the

220 considered variable *j* in the source composition (loading of this variable on the source) and another

221 (g_{ik}) defining the relative contribution of this source in that sample *i* (score of the source on this

222 sample). The sum is extended to k=1,…,p sources, leaving the measurement unexplained residual

223 stored in e_{ij}.

224 The application of factor analysis techniques to NMR spectral datasets is relatively new for

225 atmospheric sciences, though being widely employed in other fields, especially in biochemistry.

226 The most simple techniques suitable for 1D spectra allows for deconvolution into spectral profiles

227 (loadings) and corresponding contributions (scores). In the present study, we employed FA to

228 analyze the collection of 17 NMR spectra of ambient samples collected during the EUCAARI

229 campaign, and to identify and quantify major components of WSOC. The NMR data were

230 processed following the method described below.

231 The rough NMR spectra were subjected to several pre-processing steps prior to undergo to FA in

232 order to minimize spurious sources of variability. A polynomial fit was applied to the baselines and

233 subtracted from the spectra. After a careful horizontal alignment of the spectra (with the Tsp-d4

234 singlet set at chemical shift $\delta H = 0$), the peaks overlapping with blank signals were removed. The

235 spectral regions containing only sparse signals ($\delta H < 0.5$ ppm; $4.5 < \delta H < 6.5$ ppm; and $\delta H > 8.5$

ppm) were omitted. Binning over 0.02 ppm chemical shift intervals was applied to remove the effects of peak position variability caused by matrix effects. Low-resolution (400 points) spectra were finally obtained. The factor analysis methods used in this study include "Non-negative Matrix Factorization" (N-NMF) and "Multivariate Curve Resolution" (MCR), which are among most common NMR spectral unmixing techniques in many chemometric applications (Karakach et al., 2009). Two different algorithms were used for NMF, employing a projected gradient bound-constrained optimization (Lin, 2007), or a multiplicative update approach (Lee and Seung, 2001). Finally, MCR was run according to two different algorithms: the classical alternating least square approach (MCR-ALS, Tauler 1995, Jaumot et al., 2005) and a weighted alternating least square method (MCR-WALS, Wentzell et al., 2006). The mathematical goal of every model is to find values of $g_{i,k}$, $f_{k,j}$ and p that best reproduce $x_{i,j}$. For this purpose the values of $g_{i,k}$ and $f_{k,j}$ are iteratively fitted to the data using a least-squares algorithm, minimizing the fit parameter called Q. Q may be defined in different ways depending on model's approach but it is substantially always the sum of squared residuals:

$$Q^2 = \sum_{i=1}^{m} \sum_{j=1}^{n} (x_{i,j} - g_{i,k} * f_{k,j})^2$$

(2)

Unlike the classic PMF that requires an error matrix as input because its object function Q weighted the residuals by their respective uncertainties, NMF and MCR methods do not require any term referred to uncertainty and the Q-value depends only on the difference between the measurements ($x_{i,j}$) and model's results ($g_{i,k}*f_{k,j}$).

2.4 Wood burning emission experiments

A rather modern log-wood stove described in Heringa et al. (2011) was operated to sample domestic wood burning emission samples for later NMR analysis. A Dekati dilution system was used to dilute the exhaust by around a factor of 8. The flow directed on the filter was 10 liters per minute. The filters were sampled over 90 minutes and included the starting of the fire, a rather long flaming phase (with several add-ons of beech logs) and one smoldering phase at the end.

2.5 Isotopic measurements

Measurements of ^{14}C were performed on total carbon aerosols (TC) on 12 samples to obtain further source information (fossil or modern origin). The ^{14}C methodology is based on the fact that aerosols of fossil origin are completely depleted in ^{14}C due to their age, while aerosols originating from non-fossil sources (e.g. biogenic sources and biomass combustion), contains a $^{14}C/^{12}C$ ratio that can be estimated from recent atmospheric ^{14}C values. In brief, each filter sample, containing 50-80 µg of

carbon, was combusted to CO_2 in a vacuum system in the presence of pre-cleaned CuO needles (1 g; Merck pro analysis, 0.65×6 mm) (Genberg et al, 2010; Genberg et al, 2011). After purifying the evolved CO_2 cryogenically, the gas was mixed with H_2 and reduced to solid carbon using an iron catalyst at 600 °C (1 mg Fe, Merck, pro analysis, reduced, diameter 10 μm). $Mg(ClO_4)_2$ (Merck, diameter 1–4 mm) was used as a drying agent. After the reduction step (complete reaction time < 4 h) the carbon and iron catalyst were pressed into an aluminum sample holder. The sample holders containing the carbon from the aerosol samples were placed on a 40 position sample wheel together with graphitized standards (4 IAEA-C6 as primary standard; 4 IAEA-C7 and 2 OxI as secondary standards) and blanks (4 samples produced from bottled, commercial fossil CO_2). The ^{14}C analysis was performed using the single stage accelerator mass spectrometry (SSAMS) facility at Lund University (Skog, 2007; Skog et al., 2010).

The results from the ^{14}C measurements are expressed as "fraction of modern carbon" ($F^{14}C$) (Reimer et al., 2004). Carbon originating from fossil sources has a $F^{14}C$ value of 0. A $F^{14}C$ value of 1.0 represents a hypothetical concentration of naturally produced ^{14}C in atmospheric carbon from 1950, excluding anthropogenic influences. However, the atmospheric ^{14}C concentration has been altered due to emissions of fossil CO_2 (the Suess effect: decreasing the ^{14}C concentration) and due to formation of ^{14}C from testing of nuclear weapons in the late 1950ies and early 1960ies (the bomb effect: increasing the ^{14}C concentration). Due to the latter effect, the $F^{14}C$ value of atmospheric carbon dioxide in the Northern Hemisphere reached a maximum value of almost 2.0 in 1963. After the Limited Test Ban Treaty, signed in 1963, atmospheric ^{14}C began to decrease quickly, mainly due to transfer of atmospheric carbon into oceans and biosphere. In 2008, $F^{14}C$ has dropped to about 1.04 (see Genberg et al., 2011 and references therein). This value is representative for biogenic sources of carbon in 2008 and will be used in the next discussion (Sect. 5) as "reference fraction of modern carbon of biogenic aerosol" (or fM(bio)). For periods dominated by biomass burning aerosol, assumptions have to be made regarding the average age of the biomass because due to the older age of burnt wood carbonaceous aerosol from biomass burning is more enriched in ^{14}C than biogenic aerosol associated with primary biological particles (PBAP) and biogenic SOA. In the Genberg et al. (2011) paper a 60- to 80-year old tree harvested in 2008 has a $F^{14}C$ value of between 1.21 and 1.23. However, according to Gilardoni et al. (2011), the most probable $F^{14}C$ value for aerosols from biomass combustion in Po valley is 1.19. Hence this value was used here as "reference fraction of modern carbon of biomass burning aerosol" (or fM(bb)). Results of these analysis and correction of the data will be further discussed below in Sect. 5.

3 Results of the chemical analyses

3.1 Overview

Spring is a transition season in north Italy with variable weather conditions and frequent precipitation. The highest aerosol concentrations in Po valley region are typically found in the cold season when the atmosphere is more stably stratified. However, on four days among the twenty-one of the EUCAARI campaign, PM10 concentrations exceeded the 50 µg/m^3 threshold at more than one ARPA-ER stations within a set of thirteen located in an area of 100 km around San Pietro Capofiume. On 9th and 10th April, ten stations showed concentrations above 40 µg/m^3. These kind of pollution events extending over an entire sector of the Po Valley provide an example of how distributed pollution sources associated with a particular orography and under stagnant meteorological conditions lead to regional pollution events characterized by small differences in aerosol loadings between urban and rural environments. The same small differences between urban and rural areas have been observed also around Paris (Crippa et al., 2013b; Freutel et al., 2013) and Barcelona (Minguillón et al., 2011) indicating that this is probably rather common in the whole European domain.

During the first week of high-pressure conditions, the concentrations of NOx and of the non-refractory submicron aerosol components measured by the AMS exhibited sharp diurnal trends with maxima during the night and early morning (Saarikoski et al., 2012). Such behaviour is characteristic of primary or freshly produced compounds accumulating in the surface layer under a low thermal inversion and being dispersed upon formation of the mixing layer in the late morning. The HR-TOF-AMS results showed that ammonium nitrate and several of the organic fractions identified by positive matrix factorization (PMF) followed diurnal variations, while ammonium sulphate and the most oxidized fraction of particulate organic compounds ("OOA-a" in Saarikoski et al., 2012, but referring to the so called OOA-1 or LV-OOA in previous literature) showed no variations pointing to components well-mixed in the lower troposphere and therefore not linked to local sources in the Po Valley (Saarikoski et al., 2012). Among the organic fractions identified, some exhibited a low O/C ratio, namely HOA ("hydrocarbon-like compounds") which are influenced by traffic emissions, BBOA ("biomass burning organic aerosols") and N-OA ("nitrogen-containing organic aerosols"). The above three classes of organics showed diurnal trends with minima in afternoon hours and with more or less pronounced maxima in early morning or evening hours. Finally, two classes of oxygenated species, OOA-b and –c, had an oxygen-to-carbon ratio intermediate between that of BBOA and that of OOA-a, and showed complex diurnal trends. In addition, OOA-c was linked to biomass burning sources based on its downward trend in concentration observed during the campaign and based on its correlation with anhydrosugars.

337   In this paper we compare the AMS concentrations for particulate organic compounds with those

338   derived by off-line thermal (EGA, liquid-TOC) and ^{1}H-NMR analyses. Since the three techniques

339   employ different units ($\mu g/m^3$ of organic matter, of organic carbon and of organic hydrogen,

340   respectively), stoichiometric ratios must be applied for quantitative comparison. In the following

341   discussion, all concentrations of AMS factors for organic matter will be converted (using the

342   OM/OC and H/C ratios reported by Saarikoski et al. (2012)) to $\mu g/m^3$ of organic carbon ($\mu gC\ m^{-3}$)

343   for comparison with thermal analyses and of organic carbon and organic hydrogen for comparison

344   with the NMR spectroscopic data. The NMR concentrations for functional groups will be reported

345   in $\mu molH\ m^{-3}$, or upon conversion into $\mu gC\ m^{-3}$ by assuming the group-specific H/C ratios

346   introduced in previous studies (Decesari et al., 2007).

347   A quantitative comparison between AMS- and NMR-detected oxidized organic compounds

348   necessitates an examination of possible biases between the total particulate organic material

349   sampled by the filters and measured by the AMS. During the Po Valley campaign the collection

350   efficiency (CE) of the AMS was determined based on comparison with co-located off-line chemical

351   measurements: Saarikoski et al. (2012) discussed more extensively the criteria applied for the CE

352   estimation in order to correct a systematic under-prediction in absolute AMS mass concentration

353   that occurred during the first portion of the campaign (before April 9th); here we compare AMS

354   measurements with the PM1 filters collected with the dichotomous sampler and not included in the

355   analysis of Saarikoski et al. (2012). Unfortunately, only TC and not the OC/EC split was available

356   for the PM1 filters, but assuming the average EC fraction (EC/TC=25%) determined on a set of

357   filters taken in parallel (Saarikoski et al., 2012), the ratio between the total AMS organic

358   compounds, expressed in $\mu gC/m^3$, and the total OC measured on the filters was 0.97±0.30 (n=17, R

359   = 0.87) indicating no clear positive or negative biases between the two measurement systems. In

360   previous studies (Kondo et al., 2007) water-soluble organic carbon (WSOC) was attributed

361   completely to AMS OOAs while water-insoluble organics were apportioned to HOA. In the Po

362   Valley, we also had a good correlation between the organic carbon accounted for by the AMS OOA

363   factors and the WSOC determined on the filters (AMS$_{(OOAs+N-OA)}$/FiltersWSOC slope= 0.97). A

364   slightly greater slope (1.15) is obtained when including the BBOA among the AMS factors

365   contributing to the water-soluble aerosol (Fig. 1a). The average AMS/filter ratios were 0.79 and

366   0.90 for the two cases, suggesting that BBOA could contribute to WSOC, with only HOA being

367   apportioned to the water-insoluble fraction, in agreement with the findings of Kondo et al. (2007).

368   Overall, the correlation between the WSOC measured on filters and that derived from the AMS

369   factors containing heteroatoms was positive but quite scattered (R ~ 0.77). When comparing the

370   AMS oxygenated or nitrogenated organic carbon with the WSOC speciated by the NMR analysis,

371 we found a 20% excess in the AMS concentration when considering BBOA water-soluble. This can

372 be explained by the incomplete NMR characterization of the total WSOC, with an average ratio

373 between NMR and liquid-TOC analysis of 0.75±0.14 (n=17, R = 0.92). This finding is in line with

374 previous NMR measurements (Tagliavini et al. 2006) although lower with respect to the results

375 obtained during other EUCAARI field experiments in European polluted environments (manuscript

376 in preparation). Likely sources of missing carbon are compounds not carrying non-exchangeable

377 hydrogen atoms, like oxalic acid, and volatile components present in WSOC originating from

378 positive artefacts or from the hydrolysis of oligomers of low-molecular weight compounds and lost

379 during sample preparation. Another source of uncertainty is the stoichiometric H/C ratios applied to

380 the ^{1}H-NMR functional groups and that may underestimate structures having low hydrogen content.

381 For this reason, the NMR/AMS comparison was carried out also employing *organic hydrogen*

382 *concentration units* (Fig. 1d), which are determined directly by the NMR analysis without the need

383 of any conversion factors, while the AMS data are derived by applying the H/C ratios estimated by

384 high mass resolution analysis (Saarikoski et al., 2012). Fig. 1d shows again an excess of

385 concentration in the AMS data with respect to NMR, greater for hydrogen than for carbon. This

386 indicates that the non-exchangeable organic hydrogen determined by proton-NMR are a fraction of

387 the total hydrogen atoms detected by AMS and therefore the AMS - unlike NMR - accounted for at

388 least some of the acidic hydrogen atoms of H-O bonds in alcohols and carboxylic acids.

389

390 **3.2 NMR characterization of WSOC**

391 Figure 2 shows examples of ^{1}H-NMR spectra recorded during the 2008 EUCAARI experiment in

392 the Po Valley. Spectral fingerprints and individual compound speciation are in agreement with

393 previous findings in the same area (Decesari et al., 2001). Levoglucosan, methane-sulphonate and

394 four low molecular weight amines, namely monomethyl-, dimethyl-, trimethyl- and triethyl-amines

395 (MMA, DMA, TMA, TEA) were speciated and quantified. Contrary to the marine aerosol samples

396 collected on the Irish coast (Decesari et al., 2011), diethyl-amine (DEA) was not found, while TMA

397 and TEA were detected at ng/m^3 level in almost all samples (Tab. 1). The different speciation with

398 respect to the marine site probably reflects different biogenic sources, which in the Po Valley are

399 largely impacted by livestock farming and waste treatment activities (Ge et al. 2011). Wood burning

400 is an additional source of amines in the valley, but the correlations with levoglucosan

401 concentrations are negligible for most of them. With the exception of TMA, whose time trend is

402 rather flat, the other amine concentrations reach a maximum in the third period of the campaign, on

403 the days between 8 and 10th April, characterized by western Mediterranean air masses, high

404 humidity with fog occurrence and a very stratified atmosphere. We observed the highest

concentrations of ammonium nitrate in the same period, indicating that the high relative humidity may have promoted the gas-to-particle conversion of low-molecular weight amines by co-condensation with nitric acid or organic acids.

A summary of the WSOC functional group distribution is provided in Tab. 2, while a synthetic representation of its variability during the campaign is provided by Fig. 3, based on the metrics introduced by Decesari et al. (2007). Briefly, the aliphatic composition of the samples is defined by two variables: the proportion of alkoxy groups (H-C-O) and that of aliphatic groups functionalized with carbonyls or carboxyls (H-C-C=O). In addition, the ratio between NMR-detected aromatic vs aliphatic groups is visualized by dot size. Functional group concentrations are here expressed as $\mu gC/m^3$ upon applying group-specific conversion factors introduced in the paper above. Regions of the diagram assigned to broad WSOC categories, namely "SOA", biomass burning aerosol and marine aerosol, were identified on the basis of characterization of near-source samples (Decesari et al. 2007). With aim of comparison we plotted the composition of Po Valley samples discussed in Decesari et al. (2001) or collected during other experiments (unpublished data) before the EUCAARI 2008 campaign. The 2008 spring campaign samples exhibit an aliphatic composition stretching between the "biomass burning" and the "SOA" sectors with a prevalence of the latter. A clear biomass burning assignment was found for samples 04April_Night and 05April_Night, meaning that their composition is fully consistent with that recorded for samples taken in an area (Rondônia, Brazil) directly exposed to strong biomass burning emissions (Tagliavini et al. 2006).

The aromaticity of WSOC, defined again as the ratio between NMR-detected aromatic vs aliphatic groups, decreased steadily during the campaign (Fig. 3b) with a trend already observed for anhydrosugars and that can be explained by the progressive increase of minimum temperatures leading to a general decline of residential heating activities in the area (Saarikoski et al., 2012). This finding suggests that NMR-detected aromatics are mainly phenolic compounds formed by the pyrolysis of wood during combustion, together with their degradation products in the atmosphere.

The proportion of alkyl groups to the aliphatic moieties remains fairly constant resulting into a certain degree of covariance between the two main oxygenated groups, H-C-O and H-C-C=O. The conversion between hydroxylated compounds and those bearing carbonyls/carboxyls seems to be related to the air mass type and photochemical regime, since there is clear tendency to find the former at high O_3/NO_2 ratios and the latter in more photochemically-aged air masses (Fig. 3c). It should be noted that the actual change of WSOC oxidation state consequent of the "replacement" of hydroxyl- functional groups with H-C-C=O groups cannot be accurately determined based on these data, due to the uncertainty in the split between carbonyls and carboxylic groups. Examples of how

438 such speciation can be reached using proton NMR techniques are presented in the following
439 section.

440

441 **3.3 Carbonyl and carboxylic acid concentrations by NMR and AMS**

442 With the aim of a direct determination of carbonyls and carboxylic groups by proton NMR
443 spectroscopy, a total of five Andersen PM10 HiVol sample extracts, one night time and four day
444 time, underwent chemical derivatization for carbonyl and carboxylic acid determination following
445 the chemical derivatization procedures described in section 2.2. Carbonyl and carboxylic acid
446 concentrations determined with NMR were also compared with AMS measurements of fragments
447 m/z 43 ($C_2H_3O^+$) and 44 (CO_2^+) in the corresponding time periods: in fact, although we
448 acknowledge that an exact relationship between these signals and carbonyl and carboxylic acid
449 concentration has not yet been clearly established (Duplissy et al., 2011 have established a
450 relationship only for mono- and di-acids), we use here CO_2^+ and $C_2H_3O^+$ as proxies for acid and
451 non-acid oxygenated functional groups respectively. Concentrations of both functional groups from
452 NMR derivatization ranged between 0.05 to 0.15 $\mu gC/m^3$ (4 to 10 $nmol/m^3$), which is the same
453 order of magnitude derived from the AMS measurements (Tab. 3). However the carboxylic acid
454 concentrations determined by the NMR method are lower than those from AMS in most cases (Fig.
455 4) and their correlation is not good (R = 0.19). Such discrepancy could be explained by the
456 unavoidable loss of volatile carboxylic acids during the chemical derivatization procedure, or by the
457 formation of CO_2^+ fragments in the AMS vaporizer from groups other than carboxylic acids, like
458 esters and peroxides. An analogous comparison for the carbonyls shows a better correlation (R =
459 0.87) between the concentrations determined by the two techniques, although the NMR
460 methodology provides higher absolute values and slightly higher proportions to WSOC or OOA
461 carbon (Fig. 4), suggesting that the $C_2H_3O^+$ fragments in the AMS spectra do not represent the
462 totality of carbonyls (which might produce other fragments, i.e. CHO^+), although they certainly
463 account for the largest part of them.

464

465 **3.4 NMR factor analysis**

466 Four methods of factor analysis (2 NMF + 2 MCR) were applied to the series of 17 ^{1}H-NMR
467 spectra at 400-point resolution (see section 2.3). Solutions with a number of factors of two up to
468 eight were explored. The five-factors solution showed the best agreement between the four
469 algorithms in respect to both spectral profiles and contributions. With a greater number of factors,
470 strong correlations between two or more factors are found (Tab. S1), suggesting that the
471 measurements were not adequate to differentiate additional independent factors. This is also

14

472 confirmed by the analysis of the dependence of the Q values on factor number, showing a marked

473 drop until a number of five and flattening out at greater numbers of factors (Fig. S1). For more

474 details on the criteria used for choosing the factor number in NMR factor analysis see also the

475 supplementary material.

476 Figure 5 reports profiles and contributions of the 5-factors solution resulting from the four

477 algorithms. The interpretation of factor spectral profiles was based on the presence of molecular

478 resonances of tracer compounds, and on the comparison with a library of reference spectra recorded

479 in laboratory or in the field during near-source studies. The physical nature of the factors was also

480 interpreted on the basis of correlation analysis employing atmospheric tracers (Tab. 4).

481　　o NMR-Factor 1 (F1: "MSA-containing") exhibits the resonance of methane-sulphonic acid

482　　　　(MSA) at 2.81 ppm as the most characteristic peak. The peak overlaps with a background

483　　　　signal attributable to oxidized aliphatic chains. F1 air concentrations were low during the

484　　　　campaign, varying from ~ 0.00 to 0.02 μgCm^{-3}, reaching 0.06 μgCm^{-3} on the night of April

485　　　　4th. MSA is generally considered a marker for marine SOA, and its occurrence in the Po

486　　　　Valley can be explained by the proximity of the sea. This interpretation is supported by

487　　　　back-trajectory analysis, showing that during Period III of the campaign, when the highest

488　　　　concentration of F1 was observed, westerly humid air masses which had travelled over the

489　　　　west Mediterranean Sea reached the Po Valley. In the same period, however, atmospheric

490　　　　stratification promoted the increase of pollutants originating from land sources. Possible

491　　　　contributions of continental sources to MSA include the emissions of organic sulphur from

492　　　　animal husbandry and landfilling (e.g., Kim 2006), especially from pig farms, which are

493　　　　particularly diffused in the Po Valley. However, the correlation of MSA with other tracers of

494　　　　emissions from anaerobic processing of biological material remains low. In fact, factor

495　　　　analysis clearly splits between MSA and amines. F1 correlates positively with chloride but

496　　　　this cannot be fully clarified by simple chemical tracers analysis.

497　　o NMR-Factor 2 (F2: "aromatic and polyols") is characterized by a spectral profile showing

498　　　　clear signatures from aromatic compounds and polyols, closely matching the spectra of

499　　　　biomass burning aerosols obtained in laboratory (see section 4). The good correlation of F2

500　　　　contributions with the concentrations of levoglucosan and potassium (R = 0.98 and 0.71,

501　　　　respectively) supports the link between F2 and primary wood burning products. F2

502　　　　concentrations showed highest levels in Period I of the campaign with a marked diurnal

503　　　　variability with maxima at night-time, indicating production from ground-sources and

504　　　　atmospheric accumulation/dispersion governed by the diurnal cycle of the planetary

505　　　　boundary layer during days of high pressure conditions. Such pattern was already been

15

506		observed for NOx and for HOA and BBOA in the same period of the campaign (Saarikoski
507		et al., 2012).
508	o	NMR-Factor 3 and Factor 4 (F3 and F4: "polysubstituted aliphatics 1 & 2") show similar
509		spectral profiles but different time trends. Even though they could result from one single
510		factor split into two, the difference between F3 and F4 is considered real based on the fact
511		that a four-factor solution does not recombine factor 3 and 4, and it hinders the identification
512		of the other factors compared to the chosen five-factor solution. Their spectral profiles are
513		characterized by polysubstituted aliphatic moieties, some hydroxyl groups (between 3.2 and
514		4.5 ppm) with a smaller contribution from aromatics. The spectrum of F3 shows greater
515		contributions from aliphatic chains (δH ~ 1.3 ppm) and from hydroxyl groups with respect
516		to F4. Aromaticity is low, indicating that the aliphatic compounds responsible for the
517		resonances between 1.8 and 3.2 ppm are substituted mainly with carbonyls or carboxylic
518		acids. Overall, such spectral features are compatible with the composition of secondary
519		organic aerosols (SOA). F3 concentrations are greater during the (polluted) Period III of the
520		campaign, while F4 is found in all periods with little variability between polluted and
521		background conditions. F3 does not correlate with any simple chemical tracer (Tab. 4)
522		except potassium. F4 is correlated with secondary species (ammonium, sulphate, nitrate) and
523		with potassium. The correlation of potassium with F4 is much stronger than with F3, and
524		comparable to that with F2. Therefore, F4 is another candidate biomass burning factor, but,
525		given its correlation with secondary inorganic species, much more *aged* than F2, which is
526		consistent with its little correlation with levoglucosan and the functional group composition
527		dominated by carboxyls and carbonyls. The interrelationship of NMR factors F2 and F4 will
528		be discussed in more details in section 4.
529	o	NMR-Factor 5 (F5: "amines") shows the contributions from the low-molecular weight
530		amines introduced in section 3.2. Traces of MSA and unresolved aliphatic compounds
531		provide additional contributions to the spectrum of F5. Possible emissions from local
532		husbandry and agricultural practices have already been mentioned. Period III of the
533		campaign was characterized by a stably stratified atmosphere, low maximum temperatures
534		and high humidity (Saarikoski et al., 2012), with conditions favourable for the formation of
535		particulate nitrate which indeed showed the highest concentrations of the campaign in those
536		days. The correlation between F5 and aerosol nitrate suggests that the low-molecular weight
537		amines occurred in the aerosol mainly as aminium nitrate and that its formation was
538		regulated by gas/particle partitioning similarly than for ammonium nitrate

539 It should be noted that this analysis identified factors that represent extremes in the functional group

540 distributions observed for the samples (Fig. 3), with F2 showing the highest hydroxyl content

541 (lower-right corner of the diagram in Fig. 3, panel a), F3 and F4 representing compounds with the

542 highest content of aliphatic groups substituted with carbonyls and carboxyls (upper left corner), and

543 F1 and F5 accounting for the species enriched in heteroatoms (lower left corner).

544

545 **3.5 Comparison between NMR and AMS factor analyses**

546 The PMF-AMS factors for organic aerosol in San Pietro Capofiume (cf Figures 7 and 8 in

547 Saarikoski et al., 2012) were averaged over the filter sampling intervals aiming to compare with the

548 NMR factors for WSOC. The correlation coefficients between the resulting AMS factor time trends

549 and the NMR factor contributions (Fig. 5) are reported in Tab. 5. Average concentrations in

550 $molH/m^3$ and $\mu gC/m^3$ for the AMS and NMR factors in the two polluted periods and for

551 background conditions are presented in Fig. 6. The HOA contribution is excluded from this mass

552 budget as it is not expected to contribute to WSOC. As already discussed in section 3.1, there is an

553 excess of the AMS concentrations in $molH/m^3$ compared to NMR, which is not so evident when

554 using carbon concentrations (Fig. 1). This reflects the greater H/C ratios provided by the AMS

555 analysis with respect to the NMR method, as the latter is blind to hydrogen atoms bound to oxygen

556 or nitrogen atoms, which contribute to the fragments in the AMS spectra. When considering the

557 factor budget in carbon units, the total AMS concentrations exceeds the NMR concentrations only

558 in the second polluted period (or Period III), as already discussed in section 3.1.

559 The correlation analysis (Tab. 5) suggests possible overlaps between the NMR and AMS factors. In

560 particular, the NMR factor for fresh biomass burning (F2) shows strong positive correlations with

561 the AMS combustion factors (BBOA and HOA), but moderate correlations were found also with

562 OOAa, which is of secondary origin, and especially with OOAc, which is a class of oxygenated

563 aerosols associated with biomass burning (Saarikoski et al., 2012). Positive but modest correlations

564 were found also between the AMS primary combustion factors (BBOA and HOA) and the NMR

565 F4, which in turn shows the highest correlation with AMS OOAc. Therefore, there is clearly a link

566 between biomass burning and the AMS BBOA (primary) and OOAc (oxygenated), as well as with

567 the NMR factors F2 (primary) and F4 (processed). On the basis of the correlation coefficients, a

568 tentative assignment of NMR F2 to BBOA and of NMR F4 to OOAc could be postulated. The

569 functional group composition of NMR F2 indicates a much greater oxidation state than that of

570 BBOA. In fact, F2 recovers the anhydrosugars which were shown to correlate poorly with BBOA

571 while showing a more clear link with OOAc (Saarikoski et al., 2012). Therefore, the "fresh" and

572 "processed" portions of biomass burning aerosol in NMR factorization do not fully overlap with

573 those from PMF-AMS: while PMF-AMS split the two classes according to their oxygen content,
574 NMR factor analysis was more sensitive to differences in functional group distribution (phenols and
575 polyols vs. carbonyls and carboxyls).

576 Since the spectral variability and corresponding noise levels of features corresponding to different
577 functionalities are not identical between AMS and NMR, it is not surprising that the PMF factors
578 that are extracted from the two datasets are not identical. PMF solutions also generally have
579 rotational ambiguity that could result in the "fresh" and "processed" biomass burning factors being
580 separated from each other to a different extent in the two different analyses. An important
581 difference between the two methodologies is that the AMS dataset accounts for species that are
582 water-insoluble (i.e. HOA) and are not included in the NMR dataset. Finally, the different time
583 resolution of AMS and NMR data could play an important role in the PMF ability to separate
584 organic classes. Thus, AMS components often reflect not only differences in chemical composition,
585 but also differences in volatility that are likely worse resolved on the 12 hour time resolution of the
586 NMR data. Despite the differences in the individual components extracted from the AMS and
587 NMR, the correlation between the sum of fresh and aged biomass burning fractions in the AMS and
588 those from NMR analysis was very good (R = 0.89 in term of $\mu molH/m^3$ and 0.90 in term of
589 $\mu gC/m^3$, see Fig. 7). Clearly, the two techniques agreed well on the fact that two factors are needed
590 to apportion the biomass burning sources of the organic aerosol during the 2008 EUCAARI
591 campaign in the Po Valley.

592 Finally, Tab. 5 shows a positive correlation also between the AMS nitrogenated compounds (N-
593 OA) and the NMR factor for amines, indicating that aliphatic amines contributed to the nitrogen
594 content of OOA measured by the HR-TOF-AMS. The correlation is not strong, which may be
595 explained by the fact that most low-molecular weight amines can occur as nitrate salts, which are
596 semivolatile, hence prone to sampling artifacts when collected using filters. Both NMR F4 and
597 AMS N-OA occur in greater concentrations during Period III, when high relative humidities
598 favoured the partitioning of nitric acid and atmospheric volatile bases onto particles.

599

4 Contribution of biomass burning POA and SOA

601 The examination of NMR and AMS factors in search of biomass burning aerosol components led to
602 the following conclusions:

603　　1. An agreement between the NMR and AMS source apportionment for biomass burning
604　　　　aerosol could be achieved only by considering suitable lumpings of factors.

605　　2. Both NMR and AMS factor analyses suggest that biomass burning aerosols include a first
606　　　　component linked to surface sources in the Po Valley and active at night, plus a second

607   component better mixed in the atmosphere and prevalent in daytime, that can be tagged as
608   "fresh" and "aged" fractions respectively.

609   3. The AMS BBOA would then account only for the fresh component.

610   4. The split between the fresh and aged biomass burning aerosol is performed differently by
611   NMR and AMS.

612 In the present section, we compare the NMR factors obtained from our analysis with biomass

613 burning aerosols generated under laboratory conditions. At present we are able to characterize only

614 biomass burning POA using the set-up described in section 2.4. For example, the ^{1}H-NMR

615 spectrum of biomass burning aerosols generated in a log-wood stove under controlled experimental

616 conditions (Heringa et al., 2011) shows (Fig. 8a) evident resonances from aromatic moieties

617 including phenols and from hydroxylated compounds including levoglucosan, plus lower

618 proportions of other aliphatic compounds. It should be noted that levoglucosan does not account for

619 more than 15% of total hydroxyl groups indicating that they occur largely as an unresolved complex

620 mixtures, possibly including oligomers. Similar results were obtained in a smog chamber at the

621 Max Planck Institute for Chemistry during the intercomparison experiment prior to the 2002

622 SMOCC campaign (unpublished data). These data are also consistent with the spectra reported by

623 Kubatova et al. (2009), and provide confirmation that freshly produced particles, i.e., POA, account

624 for the large fraction of aromatic and hydroxylated groups typical of water-soluble biomass burning

625 aerosol (Decesari et al., 2007; Zelenay et al., 2011). In agreement with smog chamber data, we then

626 conclude that the NMR Factor 2, "aromatic & polyols", during the 2008 EUCAARI campaign

627 corresponded to biomass burning POA.

628 The spectral features of Factor 4, which we also attribute to biomass burning sources, are less

629 characteristics and their link to chemical speciation data obtained in smog chambers is less clear.

630 The spectral profile suggests a mix of aromatic compounds depleted in phenols and richer in

631 electron withdrawing substituents (like carbonylic, carboxylic or nitro-groups) mixed with a (larger)

632 fraction of aliphatic compounds substituted with unsaturated oxygenated carbon atoms, like

633 carbonyls or carboxyls but with only a few alcohols. Therefore, Factor 4 lacks compounds most

634 characteristic of fresh smoke particles like anhydrosugars and phenols. Nevertheless, carboxylic

635 acids were found in significant amounts in *ambient* biomass burning aerosols (Fig. 8b; Mayol-

636 Bracero et al., 2002; Decesari et al., 2006). Ion-exchange chromatographic techniques have been

637 applied to separate the polyol fraction of WSOC from the carboxylic acids, including the humic-like

638 substances (HULIS) in ambient smoke particles, showing that the concentration of the total acids

639 can rival with that of the alcohols (Decesari et al., 2006). We have reproduced the chromatographic

640 fractionation employed for the SMOCC biomass burning experiment in Brazil, by analysing one

641 EUCAARI sample (from 4 April, night-time) showing highest contributions of Factors 2 and 4. The

642 ^{1}H-NMR spectra recorded for the resulting chemical classes, namely neutral/basic compounds,

643 mono- and di-carboxylic acids, and polyacids (HULIS), are shown in Fig. 9. As during SMOCC,

644 the fractionation of the Po Valley sample led to a clear split of the aliphatic components of WSOC,

645 with most of the hydroxylated species and amines recovered into the neutral/basic compounds and

646 most of the aliphatic compounds substituted with carbonyls/carboxyls falling in the acidic classes.

647 The separation of the aromatic groups is less clear although the polyacids (HULIS) exhibit the

648 highest degree of aromaticity. These results support the factor analysis indicating that polyols and

649 the compounds enriched of H-C-C=O groups belong to different chemical classes, which are here

650 tagged as neutral/basic compounds and mono-/di-carboxylic acids + polyacids, respectively. The

651 comparison between factor profiles and the spectra of the chemical classes actually separated by

652 liquid chromatography indicates that the compounds responsible for Factor 4 and associated with

653 biomass burning sources but *not* correlating with levoglucosan and phenols must be searched in the

654 chemical class of mono- and di-carboxylic acids, operationally defined by the ion-exchange

655 chromatographic method.

656 During the SMOCC experiment, a greater ratio between acids with respect to polyols was found in

657 daytime hours and was attributed to the different burning conditions in the area: more smouldering

658 at night versus more active flaming in daytime (Decesari et al., 2006). During the first period of the

659 EUCAARI campaign, the same was observed in an area where biomass burning is essentially due to

660 domestic heating at night-time. An alternative explanation, more suitable for the conditions

661 encountered during EUCAARI, is that the daytime samples, richer in carboxylic acids and depleted

662 of polyols, are the result of an atmospheric processing. Ageing would trigger the observed change

663 in functional group distribution as a function of the O_3/NO_2 ratio (Fig. 3) and Factor 4 would then

664 correspond to biomass burning SOA.

665 To test the above hypothesis, more information about the NMR spectral characteristics of biomass

666 burning SOA must be collected in laboratory using smog chambers with the appropriate

667 photochemical aging. Finding "clean" fingerprints for biomass burning SOA in ambient conditions

668 can be challenging due to interfering source contributions. Best opportunities are large plumes from

669 open burning in the tropics captured after several hours of transport in the middle troposphere

670 (Capes et al., 2008). In 2007, we fortuitously captured one such events at the GAW station of

671 Monte Cimone. Smoke particles had travelled above the planetary boundary layer for 75 to 90 hours

672 from North Africa and reached the northern coast of the Mediterranean at an altitude of about 2000

673 m. For a detailed description of the event, refer to Cristofanelli et al. (2009). We discuss here the

674 NMR characteristics of the aerosol sampled in those days, as it can be considered a good example

of very aged ambient biomass burning organic aerosol. The spectrum, reported in Fig. 8c, has clearly little to do with the profile of Factor 2 and with the fingerprint of fresh smoke particles determined during the EUCAARI campaign. In fact, the composition of the Monte Cimone aged biomass burning OA lacks phenols and especially of alcohols, with levoglucosan nearly absent (as partially expected also considering the instability of levoglucosan exposed to atmospheric hydroxyl radical concentrations suggested by Hennigan et al., 2010), while aliphatic compounds polysubstituted with carbonyls/carboxyls dominate. Interestingly, the spectral profile of the Monte Cimone sample share many similarities with the polyacids (HULIS) fraction isolated from the EUCAARI sample, more than with the mono- and di-acids. These findings confirm that the compositional changes in biomass burning aerosol during long-range transport can be severe (Capes et al., 2008).

The above compilation of laboratory and ambient spectral data, although being incomplete, allows to draw first two conclusions of the nature of NMR factors linked to biomass burning POA and SOA:

1. Data from smog chambers and from ambient samplings in near-source area agree on showing large phenol and polyol contents in fresh particles (biomass burning POA).

2. Ambient data of very processed smoke particles show that phenols and polyols are strongly depleted and that aliphatic compounds substituted with carboxylic acids plus aromatics other than phenols account for the "biomass burning SOA".

3. HULIS form and enrich with ageing in biomass burning plumes. This is consistent with the fact that the aged AMS burning related factor OOAc has a higher relative intensity of m/z 44, which is a marker of carboxylic acid formation in the AMS, compared to the fresh AMS BBOA factor.

In conclusion, specific NMR fingerprints can be derived for the fresh particles (polyols and phenols) and for the very aged biomass burning aerosol (HULIS), while less distinguishing features are available for the intermediate stage of ageing, when mono- and di-carboxylic acids are formed and the composition of biomass burning SOA overlaps with that of oxidized compounds originating from other sources, like those responsible for Factor 3 during EUCAARI. Again, this observation is consistent with AMS measurements which indicate that photochemical aging of aerosols results in increased acid content and increasingly similar AMS spectra (Cubison et al., 2011; Jolleys et al., 2012). In areas impacted by residential wood burning sources, the quality of the dataset and of factor analysis will be critical for the discrimination of the NMR factor for biomass burning SOA.

5 Isotopic measurements and carbon budget

Modern and fossil fuel fractions of aerosol total carbon were measured in 12 samples during periods III, IV an V of the campaign (with methods and criteria already described in Sect. 2.5) and the results are reported in Tab. 6. Unlike period I, where the change in aerosol composition were driven by the diurnal evolution of the boundary layer, the other periods show less clear dynamics. As a result, the small changes in modern carbon fraction between samples shown by the isotopic analysis could not be related unambiguously to any of the trends of AMS and NMR factors. Aiming to estimate the contribution of modern carbon to aerosol TC from isotopic ^{14}C measurements, assumptions on the actual "reference fraction of modern carbon" have to be made. As previously discussed (see sect. 2.5), such reference value depends on the relative influence of biomass burning sources, employing 60- to 80-old tree logs as fuel, versus (strictly contemporary) biogenic sources. The two cases were considered here to provide a range of variation for $F^{14}C$ (Tab. 6). On average, $F^{14}C$ for TC was between 50% (biomass burning case) and 57% (biogenic). These results are in between the values typically observed for urban sites (Yamamoto et al., 2007; Marley et al., 2009) and those representative for rural locations (Gelencser et al., 2007; Szidat et al., 2007, Hodzic et al., 2010).

Since we have already apportioned the biomass burning fraction of OC using NMR and AMS data, in this section we employ the ^{14}C data to investigate the biogenic/anthropogenic nature of the remaining oxidized organic compounds. We have calculated an aerosol carbon budget based on the following assumptions: a) the EC/OC ratio for biomass burning aerosol was set to 0.16 based on recommendations of Szidat et al. (2006); b) amine-containing compounds and AMS N-OA originate from emissions from livestock and other modern carbon sources; c) primary OC from fossil fuel combustion is fully water-insoluble. In addition, when comparing the carbon budget based on the AMS factors with that elaborated starting from filter analysis, we attributed AMS HOA to WIOC and BBOA+OOAc to the sum of NMR F2 and F4. The resulting calculations, as campaign averages, are reported in the upper panel of Fig. 10, and, for the days covered by isotopic analysis, in the lower panels of the same figure. It can be observed that WIOC/HOA together with the fossil fraction of EC account for most of fossil TC: the totality of it, under the assumption of modern carbon dominated by biogenic emissions, leaving very little room for WSOC or OOA originating from fossil fuel combustion. As anticipated in the previous section, NMR and AMS fractionations agree in apportioning about one third of OC to biomass burning sources as a campaign average. As source intensity of wood burning decreased with time (Figures 2 and 5), the second part of the campaign, for which fossil carbon data are available, shows a lower fraction of OC apportioned to biomass burning: 20% or 22% based on respectively AMS and NMR analyses,

22

743 which fall in the range indicated by the levoglucosan analyses (from 10% to 30%, Alves et al.
744 2012).

745 Irrespectively of the hypotheses, the non-biomass burning WSOC (or OOA carbon) is prevalently
746 accounted for by modern carbon, and therefore is of *biogenic* origin. Depending on the assumptions
747 about the ^{14}C content of modern carbon, the fossil fraction of the non-biomass burning WSOC is
748 only 5 – 25%. Such biogenic nature of non-biomass burning OOA/WSOC is somewhat surprising
749 for a polluted environment at the mid-latitudes in a period of the year (March - early April) when
750 vegetation has just started to recover from winter dormancy. However, this result is in agreement
751 with known collections of ^{14}C data for atmospheric aerosols indicating a general dominance of
752 modern carbon sources including polluted areas with limited evidence of biomass burning
753 emissions (Hodzic et al., 2010).

754

755 **6 Conclusions**

756 We applied factor analysis to NMR spectroscopy for WSOC source apportionment. The 2008
757 EUCAARI campaign in the Po Valley was exceptional in respect to the variability in the aerosol
758 organic composition, due to different photochemical regimes and transport conditions. NMR factor
759 analysis identified a total of five factors. Two were associated with chemical tracers, namely MSA
760 and low-molecular weight amines. A third factor was clearly associated with primary wood burning
761 particles and showed a chemical composition dominated by anhydrosugars and other polyols and by
762 phenolic compounds. The other two factors represented "aged" components, but one of the two,
763 based on correlation with tracer compounds, was interpreted as aged biomass burning particles.
764 Similar results are provided by PMF analysis of the AMS parallel dataset. The best match between
765 total biomass burning fraction of OC estimated from the NMR was found when adding an
766 oxygenated factor to the "fresh" AMS biomass burning component (BBOA). NMR factor analysis
767 provides a differentiation between the primary oxygenated biomass burning, rich of phenols and
768 polyols, and the secondary fraction rich of carbonylic compounds and acids (including HULIS).
769 The overall change in composition between the "fresh" and "aged" biomass burning aerosol is also
770 observed in the AMS biomass burning related factors.

771 Overall, the fraction of OC apportioned to biomass burning by PMF-AMS and NMR factor analysis
772 varied between 20 and 29% (i.e., 15 to 22% of TC), in the middle-upper range of the fraction
773 estimated by molecular marker analysis (Alves et al., 2012). Most interestingly, as the ^{14}C results
774 indicate a modern fraction of TC of ca. 50-57%, carbon budget calculations imply that most of
775 unapportioned WSOC (and OOA) is from modern carbon sources, hence biogenic. Such biogenic
776 sources for OOA in a period of the year when terpene emissions are small, cannot be easily

777 explained based on the current knowledge about SOA formation mechanisms. One potential source
778 of modern carbon at the site is represented by cooking aerosols (Crippa et al., 2013b; Minguillón et
779 al., 2011; Mohr et al., 2012), which, however, were not clearly discriminated by PMF-AMS in this
780 study. On the other hand, the occurrence of methane-sulphonate and especially of amines in large
781 amounts in our samples suggest that the emission of reduced sulphur and nitrogen species provided
782 an "unconventional" (non-terpene) source of biogenic SOA in the area. Notice that part of these
783 emissions may involve anthropogenic activities, such as animal farming and waste treatment. In this
784 sense, such biogenic sources would be still anthropogenic. Clearly, the anaerobic biotic reactions
785 responsible for the emissions of amines occur according to completely different mechanisms with
786 respect to the well-studied terpene emissions from living tissues of plants. Although some recent
787 studies have examined the composition of VOCs emitted by animal farms and from their wastes,
788 their SOA formation potential is poorly known, and, on the basis of the conclusions of our study,
789 they deserve investigation.
790

795

796

797 **References**
798 Aiken, A. C., de Foy, B., Wiedinmyer, C., DeCarlo, P. F., Ulbrich, I. M., Wehrli, M. N., Szidat, S.,
799 Prevot, A. S. H., Noda, J., Wacker, L., Volkamer, R., Fortner, E., Wang, J., Laskin, A.,
800 Shutthanandan, V., Zheng, J., Zhang, R., Paredes-Miranda, G., Arnott, W. P., Molina, L. T.,
801 Sosa, G., Querol, X., and Jimenez, J. L.: Mexico city aerosol analysis during MILAGRO using high
802 resolution aerosol mass spectrometry at the urban supersite (T0) – Part 2: Analysis of the biomass
803 burning contribution and the non-fossil carbon fraction, Atmos. Chem. Phys., 10, 5315-5341,
804 doi:10.5194/acp-10-5315-2010, 2010.
805

806 Alves, C., Vicente, A., Pio, C., Kiss, G., Hoffer, A., Decesari, S., Prevot, ASH; Minguillon, MC;
807 Querol, X., Hillamo, R., Spindler, G., Swietlicki, E.: Organic compounds in aerosols from selected
808 European sites - Biogenic versus anthropogenic sources, ATMOSPHERIC ENVIRONMENT 59,
809 243-255; doi:10.1016/j.atmosenv.2012.06.013, 2012.
810

811 Barmpadimos, I., Hueglin, C., Keller, J., Henne, S., and Prévôt, A. S. H.: Influence of meteorology

812 on PM_{10} trends and variability in Switzerland from 1991 to 2008, Atmos. Chem. Phys., 11, 1813-

813 1835, doi:10.5194/acp-11-1813-2011, 2011.

814

815 Barmpadimos, I., Keller, J., Oderbolz, D., Hueglin, C., and Prevot, A. S. H.: One decade of parallel

816 fine (PM2.5) and coarse (PM10–PM2.5) particulate matter measurements in Europe: trends and

817 variability, Atmos. Chem. Phys., 12, 3189–3203, doi:10.5194/acp-12-3189-2012, 2012.

818

819 Bond, T.C., Streets, D. G., Yarber, K. F., Nelson, S. M., Woo, J.-H., Klimont, Z.: A Technology-

820 based Global Inventory of Black and Organic Carbon Emissions from Combustion, Journal of

821 Geophysical Research 109, D14203, DOI: 10.1029/2003JD003697, 2004.

822

823 Capes, G., Johnson, B., McFiggans, G., Williams, P. I., Haywood, J., and Coe H.: Aging of biomass

824 burning aerosols over West Africa: Aircraft measurements of chemical composition, microphysical

825 properties, and emission ratios, J. Geophys. Res., 113, D00C15, doi:10.1029/2008JD009845, 2008.

826

827 Crippa, M., Canonaco, F., Lanz, V. A., Äijälä, M., Allan, J. D., Carbone, S., Capes, G.,

828 Dall'Osto, M., Day, D. A., DeCarlo, P. F., Di Marco, C. F., Ehn, M., Eriksson, A., Freney, E.,

829 Hildebrandt Ruiz, L., Hillamo, R., Jimenez, J.-L., Junninen, H., Kiendler-Scharr, A.,

830 Kortelainen, A.-M., Kulmala, M., Mensah, A. A., Mohr, C., Nemitz, E., O'Dowd, C.,

831 Ovadnevaite, J., Pandis, S. N., Petäjä, T., Poulain, L., Saarikoski, S., Sellegri, K., Swietlicki, E.,

832 Tiitta, P., Worsnop, D. R., Baltensperger, U., and Prévôt, A. S. H.: Organic aerosol components

833 derived from 25 AMS datasets across Europe using a newly developed ME-2 based source

834 apportionment strategy, Atmos. Chem. Phys. Discuss., 13, 23325-23371, doi:10.5194/acpd-13-

835 23325-2013, 2013a.

836

837 Crippa, M., P. F. DeCarlo, J. G. Slowik, C. Mohr, M. F. Heringa, R. Chirico, L. Poulain, F. Freutel,

838 J. Sciare, J. Cozic, C. F. Di Marco, M. Elsasser, J. B. Nicolas, N. Marchand, E. Abidi, A.

839 Wiedensohler, F. Drewnick, J. Schneider, S. Borrmann, E. Nemitz, R. Zimmermann, J. L. Jaffrezo,

840 A. S. H. Prevot, and U. Baltensperger: Wintertime aerosol chemical composition and source

841 apportionment of the organic fraction in the metropolitan area of Paris, Atmospheric Chemistry and

842 Physics, 13(2), 961-981, 2013b.

843

844 Cristofanelli, P., Marinoni, A., Arduini, J., Bonafè, U., Calzolari, F., Colombo, T., Decesari, S.,
845 Duchi, R., Facchini, M. C., Fierli, F., Finessi, E., Maione, M., Chiari, M., Calzolai, G., Messina, P.,
846 Orlandi, E., Roccato, F., and Bonasoni, P.: Significant variations of trace gas composition and
847 aerosol properties at Mt. Cimone during air mass transport from North Africa − contributions from
848 wildfire emissions and mineral dust, Atmos. Chem. Phys., 9, 4603-4619, doi:10.5194/acp-9-4603-
849 2009, 2009.

851 Cubison, M. J., Ortega, A. M., Hayes, P. L., Farmer, D. K., Day, D., Lechner, M. J., Brune, W. H.,
852 Apel, E., Diskin, G. S., Fisher, J. A., Fuelberg, H. E., Hecobian, A., Knapp, D. J., Mikoviny, T.,
853 Riemer, D., Sachse, G. W., Sessions, W., Weber, R. J., Weinheimer, A. J., Wisthaler, A., and
854 Jimenez, J. L.: Effects of aging on organic aerosol from open biomass burning smoke in aircraft and
855 laboratory studies, Atmos. Chem. Phys., 11, 12049-12064, doi:10.5194/acp-11-12049-2011, 2011.

857 DeCarlo, P. F., Kimmel, J. R., Trimborn, A., Northway, M. J., Jayne, J. T., Aiken, A. C., Gonin,
858 M., Fuhrer, K., Horvath, T., Docherty, K. S., Worsnop, D. R., Jimenez, J. L. Field-deployable,
859 highresolution, time-of-flight aerosol mass spectrometer. Anal. Chem. 78 (24), 8281−8289, 2006.

861 Decesari S., Facchini M.C., Fuzzi S. and Tagliavini E.: Characterization of water-soluble organic
862 compounds in atmospheric aerosol: A new approach, J. Geophys. Res., 105, 1481−1489, 2000.

864 Decesari, S., Facchini, M. C., Matta, E., Lettini, F., Mircea, M., Fuzzi, S., Tagliavini, E. and
865 Putaud, J. P.: Chemical features and seasonal variation of fine aerosol water-soluble organic
866 compounds in the Po Valley, Italy, Atmos. Environ., 35, 3691−3699, 2001.

868 Decesari, S., Fuzzi, S., Facchini, M. C., Mircea, M., Emblico, L., Cavalli, F., Maenhaut, W.,
869 Chi, X., Schkolnik, G., Falkovich, A., Rudich, Y., Claeys, M., Pashynska, V., Vas, G.,
870 Kourtchev, I., Vermeylen, R., Hoffer, A., Andreae, M. O., Tagliavini, E., Moretti, F., and
871 Artaxo, P.: Characterization of the organic composition of aerosols from Rondônia, Brazil, during
872 the LBA-SMOCC 2002 experiment and its representation through model compounds, Atmos.
873 Chem. Phys., 6, 375-402, doi:10.5194/acp-6-375-2006, 2006.

875 Decesari, S., Mircea, M., Cavalli, F., Fuzzi, S., Moretti, F., Tagliavini, E. and Facchini, M. C.:
876 Source attribution of water-soluble organic aerosol by nuclear magnetic resonance spectroscopy,
877 Environ. Sci. Technol., 41, 2479−2484, 2007.

878

879 Decesari, S., Finessi, E., Rinaldi, M., Paglione, M., Fuzzi, S., Stephanou, E. G., Tziaras, T., Spyros,

880 A., Ceburnis, D., O'Dowd, C., Dall'Osto, M., Harrison, R. M., Allan, J., Coe, H., Facchini, M. C.:

881 Primary and secondary marine organic aerosols over the North Atlantic Ocean during the MAP

882 experiment, *J. Geophys. Res.*, 116, D22210, doi:10.1029/2011JD016204, 2011.

883

884 Duplissy, J., DeCarlo, P. F., Dommen, J., Alfarra, M. R., Metzger, A., Barmpadimos, I.,

885 Prevot, A. S. H., Weingartner, E., Tritscher, T., Gysel, M., Aiken, A. C., Jimenez, J. L.,

886 Canagaratna, M. R., Worsnop, D. R., Collins, D. R., Tomlinson, J., and Baltensperger, U.: Relating

887 hygroscopicity and composition of organic aerosol particulate matter, Atmos. Chem. Phys., 11,

888 1155-1165, doi:10.5194/acp-11-1155-2011, 2011.

889

890 Elsasser, M., Crippa, M., Orasche, J., DeCarlo, P. F., Oster, M., Pitz, M., Cyrys, J.,

891 Gustafson, T. L., Pettersson, J. B. C., Schnelle-Kreis, J., Prévôt, A. S. H., and Zimmermann, R.:

892 Organic molecular markers and signature from wood combustion particles in winter ambient

893 aerosols: aerosol mass spectrometer (AMS) and high time-resolved GC-MS measurements in

894 Augsburg, Germany, Atmos. Chem. Phys., 12, 6113-6128, doi:10.5194/acp-12-6113-2012, 2012.

895

896 Freutel, F., J. Schneider, F. Drewnick, S. L. von der Weiden-Reinmuller, M. Crippa, A. S. H.

897 Prevot, U. Baltensperger, L. Poulain, A. Wiedensohler, J. Sciare, R. Sarda-Esteve, J. F. Burkhart, S.

898 Eckhardt, A. Stohl, V. Gros, A. Colomb, V. Michoud, J. F. Doussin, A. Borbon, M. Haeffelin, Y.

899 Morille, M. Beekmann, and S. Borrmann: Aerosol particle measurements at three stationary sites in

900 the megacity of Paris during summer 2009: meteorology and air mass origin dominate aerosol

901 particle composition and size distribution, Atmospheric Chemistry and Physics, 13(2), 933-959,

902 2013.

903

904 Ge, X., Wexler, A. S., and Clegg, S. L.: Atmospheric amines-Part 1. A review, Atmos. Environ.,

905 45, 524–546, 2011.

906

907 Gelencsér A., Mészáros, T., Blazsó, M., Kiss, Gy., Krivácsy, Z., Molnár, A., and Mészáros, E.:

908 Structural Characterisation of Organic Matter in Fine Tropospheric Aerosol by Pyrolysis-Gas

909 Chromatography-Mass Spectrometry, Journal of Atmospheric Chemistry, Volume 37, Number 2

910 (2000), 173-183, DOI: 10.1023/A:1006402731340. 2000.

911

912 Gelencsér, A., May, B., Simpson, D., Sánchez-Ochoa, A., Kasper-Giebl, A., Puxbaum, H., Caseiro,
913 A., Casimiro, P., and Legrand, M.: Source apportionment of PM2.5 organic aerosol over Europe:
914 Primary/secondary, natural/anthropogenic, and fossil/biogenic origin, Journal of Geophysical
915 Research: Atmospheres, 112, D23, 1984–2012, DOI: 10.1029/2006JD008094, 2007.

916

917 Genberg, J., Stenström, K., Elfman, M., and Olsson, M: Development of graphitization of μg-sized
918 samples at Lund University, Radiocarbon, 52, 1270-1276, 2010.

919

920 Genberg, J., Hyder, M., Stenström, K., Bergström, R., Fors, E., Jönsson, J.Å., and Swietlicki, E.:
921 *Source apportionment of carbonaceous aerosol in Southern Sweden,* Atmos. Chem. Phys., 11,
922 11387-11400, DOI:10.5194/acp-11-11387-2011, 2011.

923

924 Gilardoni S., Vignati E., Cavalli F., Putaud J.P., Larsen B.R., Karl M., Stenström K., Genberg J.,
925 Henne S., and Dentener F.: Better constraints on sources of carbonaceous aerosols using a
926 combined 14C – macro tracer analysis in a European rural background site, Atmos. Chem. Phys.,
927 11, 5685-5700, doi:10.5194/acp-11-5685-2011, 2011.

928

929 Hallquist, M., Wenger, J. C., Baltensperger, U., Rudich, Y., Simpson, D., Claeys, M., Dommen, J.,
930 Donahue, N. M., George, C., Goldstein, A. H., Hamilton, J. F., Herrmann, H., Hoffmann, T.,
931 Iinuma, Y., Jang, M., Jenkin, M. E., Jimenez, J. L., Kiendler-Scharr, A., Maenhaut, W.,
932 McFiggans, G., Mentel, Th. F., Monod, A., Prévôt, A. S. H., Seinfeld, J. H., Surratt, J. D.,
933 Szmigielski, R. and Wildt, J.: The formation, properties and impact of secondary organic aerosol:
934 current and emerging issues, Atmos. Chem. Phys., 9, 5155-5236, doi:10.5194/acp-9-5155-2009,
935 2009.

936

937 Hand, J. L., Schichtel, B. A., Malm, W. C., and Pitchford, M. L.: Particulate sulfate ion
938 concentration and SO_2 emission trends in the United States from the early 1990s through 2010,
939 Atmos. Chem. Phys., 12, 10353-10365, doi:10.5194/acp-12-10353-2012, 2012.

940

941 Hennigan, C. J., A. P. Sullivan, J. L. Collett Jr., and A. L. Robinson: Levoglucosan stability in
942 biomass burning particles exposed to hydroxyl radicals, Geophys. Res. Lett., 37, L09806,
943 doi:10.1029/2010GL043088, 2010.

944

945   Harrison, R. M., Yin, J.: Sources and processes affecting carbonaceous aerosol in central England,

946   Atmospheric Environment, 42-7, 1413-1423, doi:10.1016/j.atmosenv.2007.11.004, 2008.

947

948   Heringa, M. F., DeCarlo, P. F., Chirico, R., Tritscher, T., Dommen, J., Weingartner, E., Richter, R.,

949   Wehrle, G., Prévôt, A. S. H., and Baltensperger, U.: Investigations of primary and secondary

950   particulate matter of different wood combustion appliances with a high-resolution time-of-flight

951   aerosol mass spectrometer, Atmos. Chem. Phys., 11, 5945-5957, doi:10.5194/acp-11-5945-2011,

952   2011.

953

954   Heringa, M. F., DeCarlo, P. F., Chirico, R., Tritscher, T., Clairotte, M., Mohr, C., Crippa, M.,

955   Slowik, J. G., Pfaffenberger, L., Dommen, J., Weingartner, E., Prévôt, A. S. H., and

956   Baltensperger, U.: A new method to discriminate secondary organic aerosols from different sources

957   using high-resolution aerosol mass spectra, Atmos. Chem. Phys., 12, 2189-2203, doi:10.5194/acp-

958   12-2189-2012, 2012.

959

960   Hodzic, A., Jimenez, J. L., Prévôt, A. S. H., Szidat, S., Fast, J. D., and Madronich, S.: Can 3-D

961   models explain the observed fractions of fossil and non-fossil carbon in and near Mexico City?,

962   Atmos. Chem. Phys., 10, 10997-11016, doi:10.5194/acp-10-10997-2010, 2010..

963

964   Jaumot, J., Gargallo, R., de Juan, A., Tauler, R.: A graphical user-friendly interface for MCR-ALS:

965   a new tool for multivariate curve resolution in MATLAB, Chemometrics And Intelligent

966   Laboratory Systems, 76(1), 101-110, May 2005.

967

968   Jolleys, M. D., Coe, H., McFiggans, G., Capes, G., Allan, J. D. , Crosier, J., Williams, P. I., Allen,

969   G., Bower, K. N., Jimenez, J. L., Russell, L. M., Grutter, M., and Baumgardner, D.: Characterizing

970   the Aging of Biomass Burning Organic Aerosol by Use of Mixing Ratios: A Meta-analysis of Four

971   Regions, *Environ. Sci. Technol.*, 46 (24), pp 13093–13102, 2012.

972

973   Karakach, T. ,K., Knight, R., Lenz E. M., Viant, M. R., Walter, J. A.: Analysis of time course [1]H

974   NMR metabolomics data by multivariate curve resolution, Magn Reson Chem. 2009 Dec;47 Suppl

975   1:S105-17, 2009.

976

977   Kiendler-Scharr A., Zhang Q., Hohaus T., Kleist E., Mensah A., Mentel T., Spindler C., Uerlings

978   R., Tillmann R. and Wildt J.: Aerosol Mass Spectrometric Features of Biogenic SOA: Observations

979 from a Plant Chamber and in Rural Atmospheric Environments, Environ. Sci. Technol. 43, 8166–
980 8172, 2009.

981

982 Kim, K. H.: Emissions of reduced sulfur compounds (RSC) as a landfill gas (LFG): a comparative
983 study of young and old landfill facilities, Atmospheric Environment 40, 6567-6578, 2006.

984

985 Kondo, Y. , Miyazaki, Y., Takegawa, N., Miyakawa, T., Weber, R. J., Jimenez, J. L., Zhang, Q. and
986 Worsnop, D.R.: Oxygenated and water-soluble organic aerosols in Tokyo, Journal of Geophysical
987 Research, 112, p. D011203 http://dx.doi.org/10.1029/2006JD007056, 2007.

988

989 Kubátová A., Lahren T.J., Beránek J., Smoliakova I.P., Braun A. and Huggins F.E.: Extractable
990 Organic Carbon and its Differentiation by Polarity in Diesel Exhaust, Wood Smoke, and Urban
991 Particulate   Matter,   Aerosol   Science   and   Technology,   43(7),   714-729,   DOI:
992 10.1080/02786820902889853, 2009.

993

994 Kulmala, M., Asmi, A., Lappalainen, H. K., Baltensperger, U., Brenguier, J.-L., Facchini, M. C.,
995 Hansson, H.-C., Hov, Ø., O'Dowd, C. D., Pöschl, U., Wiedensohler, A., Boers, R., Boucher, O.,
996 de Leeuw, G., Denier van der Gon, H. A. C., Feichter, J., Krejci, R., Laj, P., Lihavainen, H.,
997 Lohmann, U., McFiggans, G., Mentel, T., Pilinis, C., Riipinen, I., Schulz, M., Stohl, A.,
998 Swietlicki, E., Vignati, E., Alves, C., Amann, M., Ammann, M., Arabas, S., Artaxo, P., Baars, H.,
999 Beddows, D. C. S., Bergström, R., Beukes, J. P., Bilde, M., Burkhart, J. F., Canonaco, F.,
1000 Clegg, S. L., Coe, H., Crumeyrolle, S., D'Anna, B., Decesari, S., Gilardoni, S., Fischer, M.,
1001 Fjaeraa, A. M., Fountoukis, C., George, C., Gomes, L., Halloran, P., Hamburger, T.,
1002 Harrison, R. M., Herrmann, H., Hoffmann, T., Hoose, C., Hu, M., Hyvärinen, A., Hõrrak, U.,
1003 Iinuma, Y., Iversen, T., Josipovic, M., Kanakidou, M., Kiendler-Scharr, A., Kirkevåg, A., Kiss, G.,
1004 Klimont, Z., Kolmonen, P., Komppula, M., Kristjánsson, J.-E., Laakso, L., Laaksonen, A.,
1005 Labonnote, L., Lanz, V. A., Lehtinen, K. E. J., Rizzo, L. V., Makkonen, R., Manninen, H. E.,
1006 McMeeking, G., Merikanto, J., Minikin, A., Mirme, S., Morgan, W. T., Nemitz, E., O'Donnell, D.,
1007 Panwar, T. S., Pawlowska, H., Petzold, A., Pienaar, J. J., Pio, C., Plass-Duelmer, C.,
1008 Prévôt, A. S. H., Pryor, S., Reddington, C. L., Roberts, G., Rosenfeld, D., Schwarz, J., Seland, Ø.,
1009 Sellegri, K., Shen, X. J., Shiraiwa, M., Siebert, H., Sierau, B., Simpson, D., Sun, J. Y., Topping, D.,
1010 Tunved, P., Vaattovaara, P., Vakkari, V., Veefkind, J. P., Visschedijk, A., Vuollekoski, H.,
1011 Vuolo, R., Wehner, B., Wildt, J., Woodward, S., Worsnop, D. R., van Zadelhoff, G.-J.,
1012 Zardini, A. A., Zhang, K., van Zyl, P. G., Kerminen, V.-M., S Carslaw, K., and Pandis, S. N.:

General overview: European Integrated project on Aerosol Cloud Climate and Air Quality interactions (EUCAARI) – integrating aerosol research from nano to global scales, Atmos. Chem. Phys., 11, 13061-13143, doi:10.5194/acp-11-13061-2011, 2011.

Lanz, V. A., Alfarra, M. R., Baltensperger, U., Buchmann, B., Hueglin, C., and Prévôt, A. S. H.: Source apportionment of submicron organic aerosols at an urban site by factor analytical modelling of aerosol mass spectra, Atmos. Chem. Phys., 7, 1503–1522, 2007.

Lee D., Seung H., Algorithms for non-negative matrix factorization. Adv. Neural Inform. Process. Systems 13, 556-562, 2001.

Lin, C.-J.: Projected Gradient methods for Non-negative matrix factorization. Neural Computation, 19, 2756-2779, 2007.

Mancinelli, V., Rinaldi, M., Finessi, E., Emblico, L., Mircea, M., Fuzzi, S., Facchini, M. C., Decesari, S.: An anion-exchange high-performance liquid chromatography method coupled to total organic carbon determination for the analysis of water-soluble organic aerosols, J. Chromatogr. A., 18; 1149(2):385-9, 16, 2007.

Manninen, H. E., Nieminen, T., Asmi, E., Gagné, S., Häkkinen, S., Lehtipalo, K., Aalto, P., Vana, M., Mirme, A., Mirme, S., Hõrrak, U., Plass-Dülmer, C., Stange, G., Kiss, G., Hoffer, A., Törő, N., Moerman, M., Henzing, B., de Leeuw, G., Brinkenberg, M., Kouvarakis, G. N., Bougiatioti, A., Mihalopoulos, N., O'Dowd, C., Ceburnis, D., Arneth, A., Svenningsson, B., Swietlicki, E., Tarozzi, L., Decesari, S., Facchini, M. C., Birmili, W., Sonntag, A., Wiedensohler, A., Boulon, J., Sellegri, K., Laj, P., Gysel, M., Bukowiecki, N., Weingartner, E., Wehrle, G., Laaksonen, A., Hamed, A., Joutsensaari, J., Petäjä, T., Kerminen, V.-M., and Kulmala, M.: EUCAARI ion spectrometer measurements at 12 European sites – analysis of new particle formation events, Atmos. Chem. Phys., 10, 7907-7927, doi:10.5194/acp-10-7907-2010, 2010.

Mayol-Bracero, O. L., Guyon, P., Graham, B., Roberts, G., Andreae, M. O., Decesari, S., Facchini, M. C., Fuzzi, S., and Artaxo, P.: Water-soluble organic compounds in biomass burning aerosols over Amazonia 2. Apportionment of the chemical composition and importance of the polyacidic fraction, *J. Geophys. Res.*, 107(D20), 8091, doi:10.1029/2001JD000522, 2002.

1047

1048 Marley, N. A., Gaffney, J. S., Tackett, M., Sturchio, N. C., Heraty, L., Martinez, N., Hardy, K. D.,
1049 Marchany-Rivera, A., Guilderson, T., MacMillan, A., and Steelman, K.: The impact of biogenic
1050 carbon sources on aerosol absorption in Mexico City, Atmos. Chem. Phys., 9, 1537-1549,
1051 doi:10.5194/acp-9-1537-2009, 2009.

1052

1053 Mohr, C., DeCarlo, P. F., Heringa, M. F., Chirico, R., Slowik, J. G., Richter, R., Reche, C.,
1054 Alastuey, A., Querol, X., Seco, R., Peñuelas, J., Jiménez, J. L., Crippa, M., Zimmermann, R.,
1055 Baltensperger, U., and Prévôt, A. S. H.: Identification and quantification of organic aerosol from
1056 cooking and other sources in Barcelona using aerosol mass spectrometer data, Atmos. Chem. Phys.,
1057 12, 1649-1665, 2012.

1058

1059 Minguillón, M. C., Perron, N., Querol, X., Szidat, S., Fahrni, S. M., Alastuey, A., Jimenez, J. L.,
1060 Mohr, C., Ortega, A. M., Day, D. A., Lanz, V. A., Wacker, L., Reche, C., Cusack, M., Amato, F.,
1061 Kiss, G., Hoffer, A., Decesari, S., Moretti, F., Hillamo, R., Teinilä, K., Seco, R., Peñuelas, J.,
1062 Metzger, A., Schallhart, S., Müller, M., Hansel, A., Burkhart, J. F., Baltensperger, U., and
1063 Prévôt, A. S. H.: Fossil versus contemporary sources of fine elemental and organic carbonaceous
1064 particulate matter during the DAURE campaign in Northeast Spain, Atmos. Chem. Phys., 11,
1065 12067-12084, doi:10.5194/acp-11-12067-2011, 2011.

1066

1067 Moretti, F., Tagliavini, E., Decesari, S., Facchini, M. C., Rinaldi, M., Fuzzi, S.: NMR determination
1068 of total carbonyls and carboxyls: a tool for tracing the evolution of atmospheric oxidized organic
1069 aerosols, Environ Sci Technol., 42(13):4844-9, 2008.

1070

1071 Nordin, E. Z., Eriksson, A. C., Roldin, P., Nilsson, P. T., Carlsson, J. E., Kajos, M. K., Hellén, H.,
1072 Wittbom, C., Rissler, J., Löndahl, J., Swietlicki, E., Svenningsson, B., Bohgard, M., Kulmala, M.,
1073 Hallquist, M., and Pagels, J. H.: Secondary organic aerosol formation from idling gasoline
1074 passenger vehicle emissions investigated in a smog chamber, Atmos. Chem. Phys., 13, 6101-6116,
1075 doi:10.5194/acp-13-6101-2013, 2013.

1076

1077 Reimer, P.J., Brown, T.A. and Reimer, R.W.: Discussion: reporting and calibration of post-bomb
1078 ^{14}C data, Radiocarbon, 46(3), 1299–304, 2004.

1079

1080 Rinaldi M., Emblico L., Decesari S., Fuzzi S., Facchini M. C., Librando V.: Chemical
1081 characterization and source apportionment of size-segregated aerosol collected at an urban site in
1082 Sicily, Water Air Soil Pollut., 185, 311-321. DOI 10.1007/s11270-007-9455-4, 2007.

1083

1084 Robinson, A. L., Donahue, N. M., Shrivastava, M. K., Weitkamp, E. A., A. M. Sage, Grieshop, A.
1085 P., Lane, T. E., Pierce, J. R., Pandis, S. N.: Rethinking organic aerosols: Semivolatile emissions and
1086 photochemical aging. Science 315:1259–1262, 2007.

1087

1088 Saarikoski, S., Carbone, S., Decesari, S., Giulianelli, L., Angelini, F., Canagaratna, M., Ng, N. L.,
1089 Trimborn, A., Facchini, M. C., Fuzzi, S., Hillamo, R., and Worsnop, D.: Chemical characterization
1090 of springtime submicrometer aerosol in Po Valley, Italy, Atmos. Chem. Phys., 12, 8401-8421,
1091 doi:10.5194/acp-12-8401-2012, 2012.

1092

1093 Skog, G.: The single stage AMS machine at Lund University: Status report, Nucl. Instr. Meth. B,
1094 259(1), 1–6, 2007.

1095

1096 Skog, G., Rundgren, M., and Sköld, P.: Status of the Single Stage AMS machine at Lund University
1097 after 4 years of operation, Nucl. Instr. Meth. B, 268(7–8), 895–97, 2010.

1098

1099 Szidat, S., Jenk, T. M., Synal, H.-A., Kalberer, M., Wacker, L., Hajdas, I., Kasper-Giebl, A., and
1100 Baltensperger, U.: Contributions of fossil fuel, biomass burning, and biogenic emissions to
1101 carbonaceous aerosols in Zurich as traced by 14C, J. Geophys. Res., 111, D07206,
1102 doi:10.1029/2005JD006590, 2006.

1103

1104 Szidat, S., Prévôt, A. S. H., Sandradewi, J., Alfarra, M. R., Synal, H.- A., Wacker, L., and
1105 Baltensperger, U.: Dominant impact of residential wood burning on particulate matter in Alpine
1106 valleys during winter, Geophys. Res. Lett., 34, L05820, doi:10.1029/2006GL028325, 2007.

1107

1108 Tagliavini, E., Moretti, F., Decesari, S., Facchini, M. C., Fuzzi, S., and Maenhaut, W.: Functional
1109 group analysis by H NMR/chemical derivatization for the characterization of organic aerosol from
1110 the SMOCC field campaign, Atmos. Chem. Phys., 6, 1003-1019, doi:10.5194/acp-6-1003-2006,
1111 2006.

1112

1113   Tauler R., Multivariate Curve Resolution applied to second order data. Chemometrics and
1114   Intelligent Laboratory Systems 30, 133-146, 1995.

1115

1116   Terrado, M., Barcelo D., Tauler R., Multivariate curve resolution of organic pollution patterns in
1117   the Ebro River surface water-groundwater-sediment-soil system, ANALYTICA CHIMICA
1118   ACTA Volume: 657 Issue: 1 Pages: 19-27 DOI: 10.1016/j.aca.2009.10.026, 2010.

1119

1120   Viana, M., Kuhlbusch, T. A. J., Querol, X., Alastuey, A., Harrison, R. M., Hopke, P. K.,
1121   Winiwarter, W., Vallius, M., Szidat, S., Prévôt, A. S. H., Hueglin, C., Bloemen, H., Wåhlin, P.,
1122   Vecchi, R., Miranda, A. I., Kasper-Giebl, A., Maenhaut, W., Hitzenberger, R.: Source
1123   apportionment of particulate matter in Europe: a review of methods and results, *J. Aerosol Sci.* 39:
1124   827–849, 2008.

1125

1126   Wentzell, P. D., Karakach, T. K., Roy, S., Martinez, M. J., Allen, C. P., Werner-Washburne, M.:
1127   Multivariate curve resolution of time course microarray data.BMC Bioinformatics 7, 343, 2006.

1128

1129   Yamamoto, N., Muramoto, A., Yoshinaga, J., Shibata, K., Endo, M., Endo, O., Hirabayashi, M.,
1130   Tanabe, K., Goto, S., Yoneda, M., Shibata Y.: Comparison of carbonaceous aerosols in Tokyo
1131   before and after implementation of diesel exhaust restrictions, Environ Sci Technol.
1132   15;41(18):6357-62, 2007.

1133

1134   Zelenay, V., R. Mooser, T. Tritscher, A. Křepelová, M. F. Heringa, R. Chirico, A. S. H. Prévôt, E.
1135   Weingartner, U. Baltensperger, J. Dommen, B. Watts, J. Raabe, T. Huthwelker, and M. Ammann:
1136   Aging induced changes on NEXAFS fingerprints in individual combustion particles, Atmos. Chem.
1137   Phys., 11(22), 11777-11791, 2011.

1138

1139   Zhang, Q., Worsnop, D. R., Canagaratna, M. R., and Jimenez, J. L.: Hydrocarbon-like and
1140   oxygenated organic aerosols in Pittsburgh: insights into sources and processes of organic aerosols,
1141   Atmos. Chem. Phys., 5, 3289-3311, doi:10.5194/acp-5-3289-2005, 2005.

1142

1143

1144

1145

Tables and Figures

Tab. 1: Concentrations (ng/m^3) of alkyl amines as measured by ^{1}H-NMR spectra.

	MMA	DMA	TMA	TEA
Period I (n = 7)	3	6	2	3
Period III (n = 6)	5	8	1	30
Periods II+ IV+V (n= 4)	1	3	1	6
all campaign	3	6	1	13

Tab. 2: Average functional group concentrations as nmolH/m^3 and µgC/m^3 in the different periods of the campaign and for the whole experiment

	nmol H/m^3						±µgC/m^3						
	H-Ar	H-C-O	MSA	HC-N	H-C-C=	H-C	H-Ar	H-C-O	MSA	HC-N	H-C-(C=)	(H-C)-C=O	H-C
Period I (n = 7)	7.9	16.0	0.3	1.6	36	42	0.24	0.17	0.00	0.01	0.21	0.17	0.25
Period III (n = 6)	5.5	16.2	0.9	3.5	38	55	0.17	0.18	0.00	0.02	0.23	0.20	0.33
Periods II+ IV+V (n= 4)	2.1	7.3	0.3	1.0	19	29	0.06	0.08	0.00	0.01	0.11	0.10	0.17
all campaign	5.7	14.0	0.5	2.2	33	43	0.17	0.15	0.00	0.01	0.20	0.17	0.26

Tab. 3: COOH and carbonyl concentrations from AMS and derivatization – ^{1}H-NMR analysis. All concentrations in µgC/m^3. AMS OOC stands for the carbon concentrations of all OOA types + BBOA.

Sample	NMR			AMS		
	WSOC	COOH	C=O	OOC	fragment CO_2^+	fragment $C_2H_3O^+$
3103N	2.15	0.10	0.13	2.93	0.26	0.069
1404D	1.36	0.05	0.08	0.55	0.092	0.019
1604D	1.17	0.07	0.06	0.79	0.098	0.025
1704D	1.22	0.15	0.06	0.91	0.11	0.028
1904D	1.32	0.08	0.10	1.27	0.16	0.06

1161 **Tab. 4**: Pearson correlation coefficients (R) between NMR WSOC factors and simple chemical tracers. Only R values >
1162 0.3 are shown.

	Cl$^-$	NO$_3^-$	SO$_4^{2-}$	Na$^+$	NH$_4^+$	K$^+$	Levoglucosan
NMR Factor 1							
NMR Factor 2					0.30	0.71	0.98
NMR Factor 3						0.33	
NMR Factor 4		0.55	0.68	0.37	0.57	0.69	
NMR Factor 5	0.58	0.45	0.45		0.50		

1163

1164

1165 **Tab. 5**: Correlation matrix between NMR and AMS factors. Only R values > 0.3 are shown.

	OOAc	N-OA	OOAa	OOAb	HOA	BBOA
NMR Factor 1				0.51		
NMR Factor 2	0.74		0.57		0.85	0.79
NMR Factor 3		0.45	0.43			0.34
NMR Factor 4	0.78				0.36	0.32
NMR Factor 5		0.50		0.63		

1166
1167
1168
1169
1170
1171
1172
1173
1174
1175
1176
1177
1178
1179
1180
1181
1182
1183
1184
1185

Tab. 6: Results of ^{14}C analysis. The activities of the samples taken directly from the measurements ($F^{14}C$) are reported together with their experimental errors. The percentages of modern carbon with respect to the total were calculated taking into account two different scenarios: one in which we considered the modern carbon completely coming from biogenic aerosol (using fM(bio)=1.04) and the second one in which we considered the modern carbon entirely derived by biomass burning aerosol (using fM(bb)=1.19).

Sample ID	$F^{14}C$	% modern $C_{(BB)}$	% modern $C_{(BIO)}$
08/04_D	0.608 ± 0.011	51%	58%
08/04_N	0.704 ± 0.014	59%	68%
09/04_D	0.542 ± 0.011	46%	52%
09/04_N	0.588 ± 0.014	49%	57%
10/04_D	0.558 ± 0.014	47%	54%
10/04_N	0.588 ± 0.011	49%	57%
11/04_D	0.534 ± 0.011	45%	51%
11/04_N	0.573 ± 0.011	48%	55%
12/04_D	0.536 ± 0.010	45%	52%
12/04_N	0.738 ± 0.014	62%	71%
13/04_D	0.609 ± 0.011	51%	59%
14/04_D	0.572 ± 0.011	48%	55%
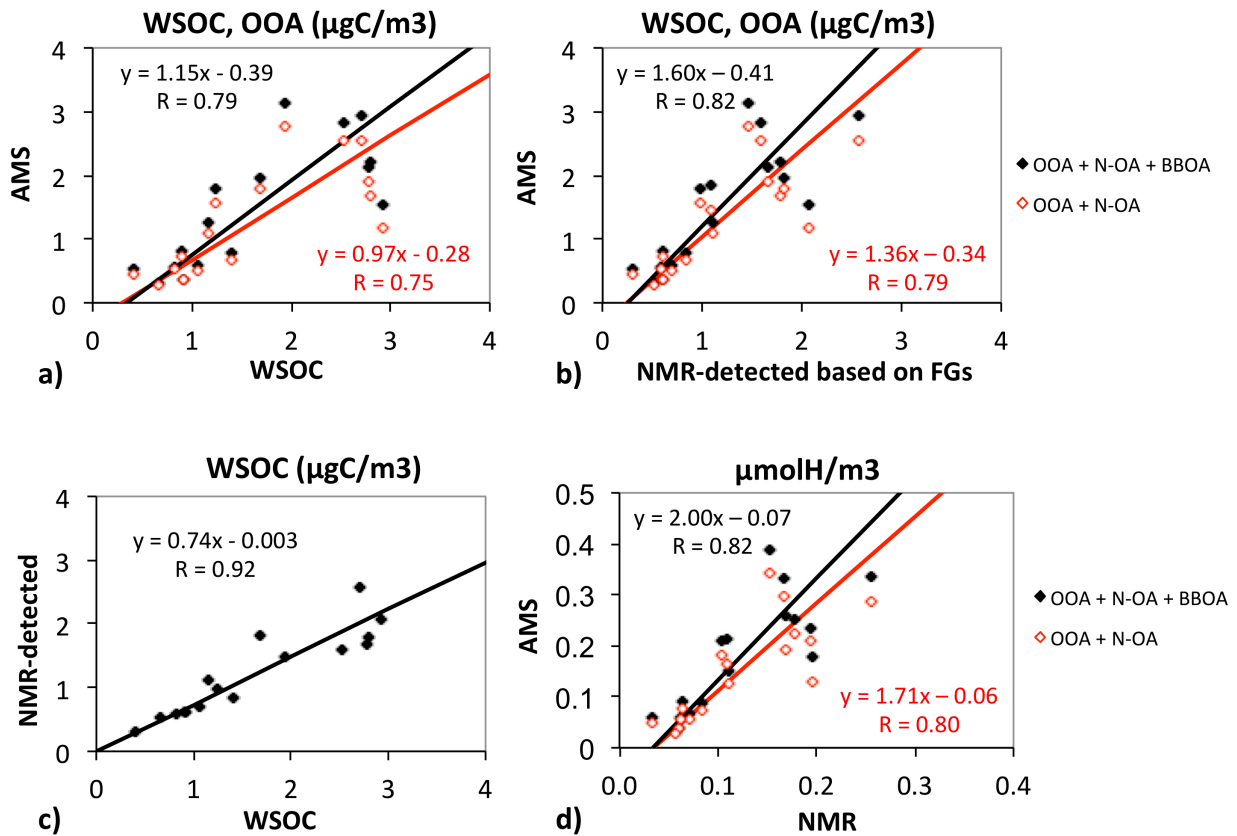
Fig. 1: a), b), c) Orthogonal fitting between carbon classes derived from TOC analysis, AMS measurements and ^{1}H-NMR analysis. d) Scatter plot (with orthogonal linear fit again) between AMS and ^{1}H-NMR concentrations of organic hydrogen.
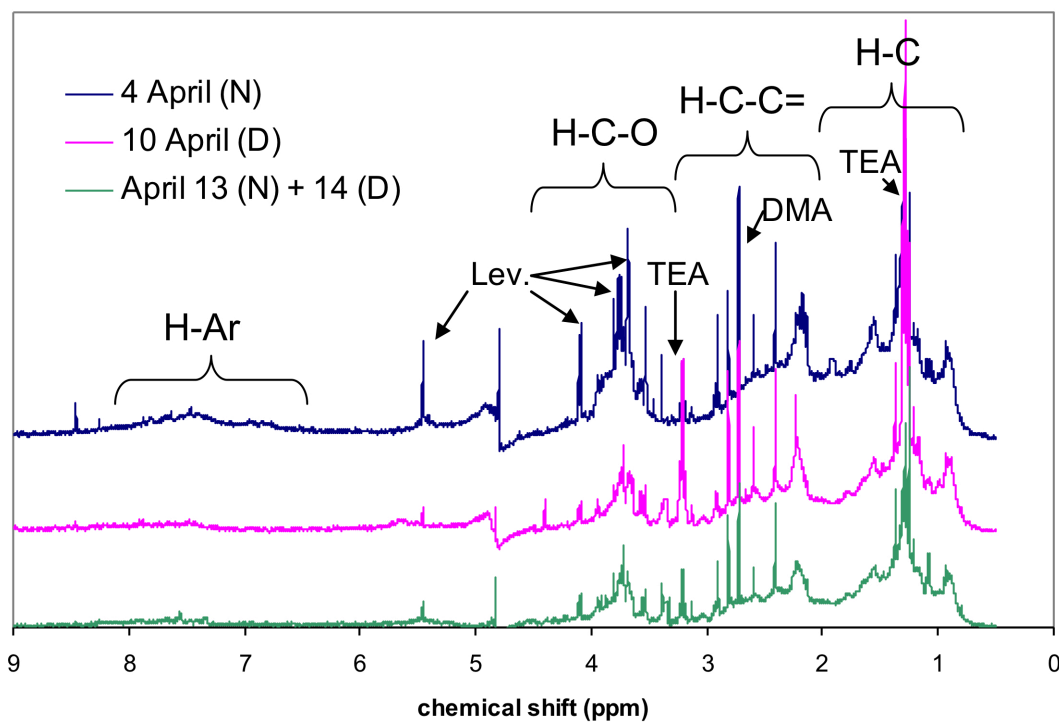
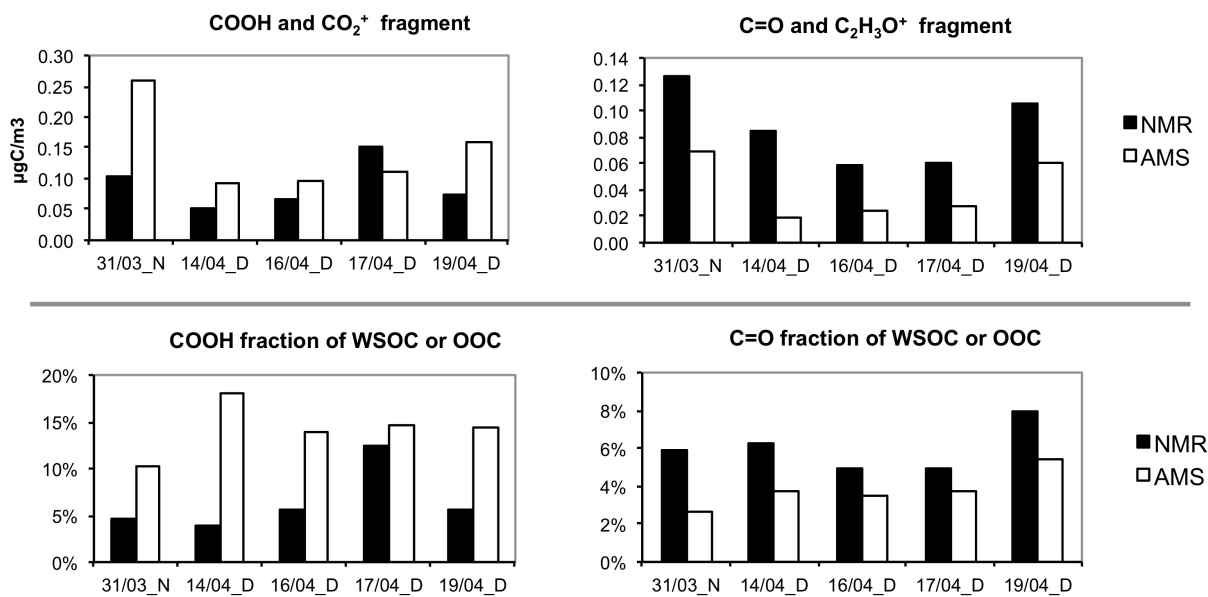**Fig. 2**: Examples of ^{1}H-NMR spectra of different aerosol SPC 2008 EUCAARI samples.
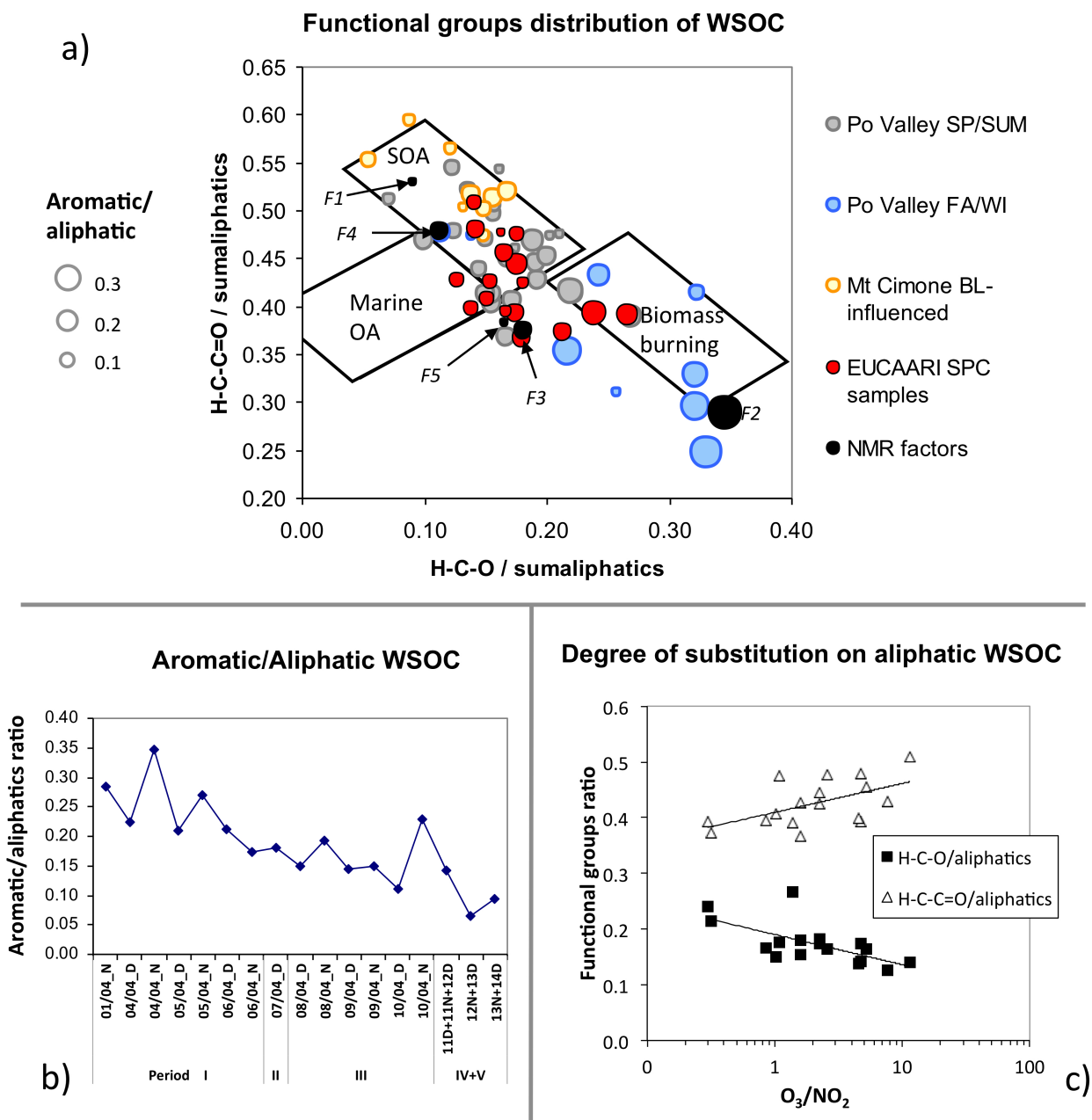
Fig. 3: a) ^{1}H-NMR functional groups distribution of the SPC 2008 EUCAARI samples compared to submicron aerosol compositions derived from previous studies in the same area. Black dots represent the functional groups distribution of the NMR factors derived from the factor analysis described in the following section 3.4. b) Time trend of aromaticity (defined as the ratio between aromatics and the sum of aliphatic groups). c) Relative content of oxygenated aliphatic functional groups as a function of trace gas composition.

COOH and CO₂⁺ fragment

C=O and C₂H₃O⁺ fragment

COOH fraction of WSOC or OOC

C=O fraction of WSOC or OOC

1209

1210   **Fig. 4**: Concentration of carboxylic acids and carbonyls determined by chemical derivatization – ^{1}H-NMR analysis in

1211   five PM1 WSOC samples. Time-averaged concentrations of the fragment CO_2^+ fragment $C_2H_3O^+$ from HR-TOF-AMS

1212   measurements are also reported as proxies for acid and non-acid oxygenated functional groups respectively. For more

1213   details refer to the text.

Fig. 5 profiles and contributions of 5-factors solution from ^{1}H-NMR spectra factor analysis. Results from all 4 different algorithms were reported: Projected Gradient (red line), Multiplicative (green line), MCR-ALS (orange line) and MCR-WALS (violet line). Signal intensity of the spectral profiles was normalized (integral=1). The samples suffixes indicate "day-time" (_D) and "night-time" (_N) sampled filters. For more details refer to the text.
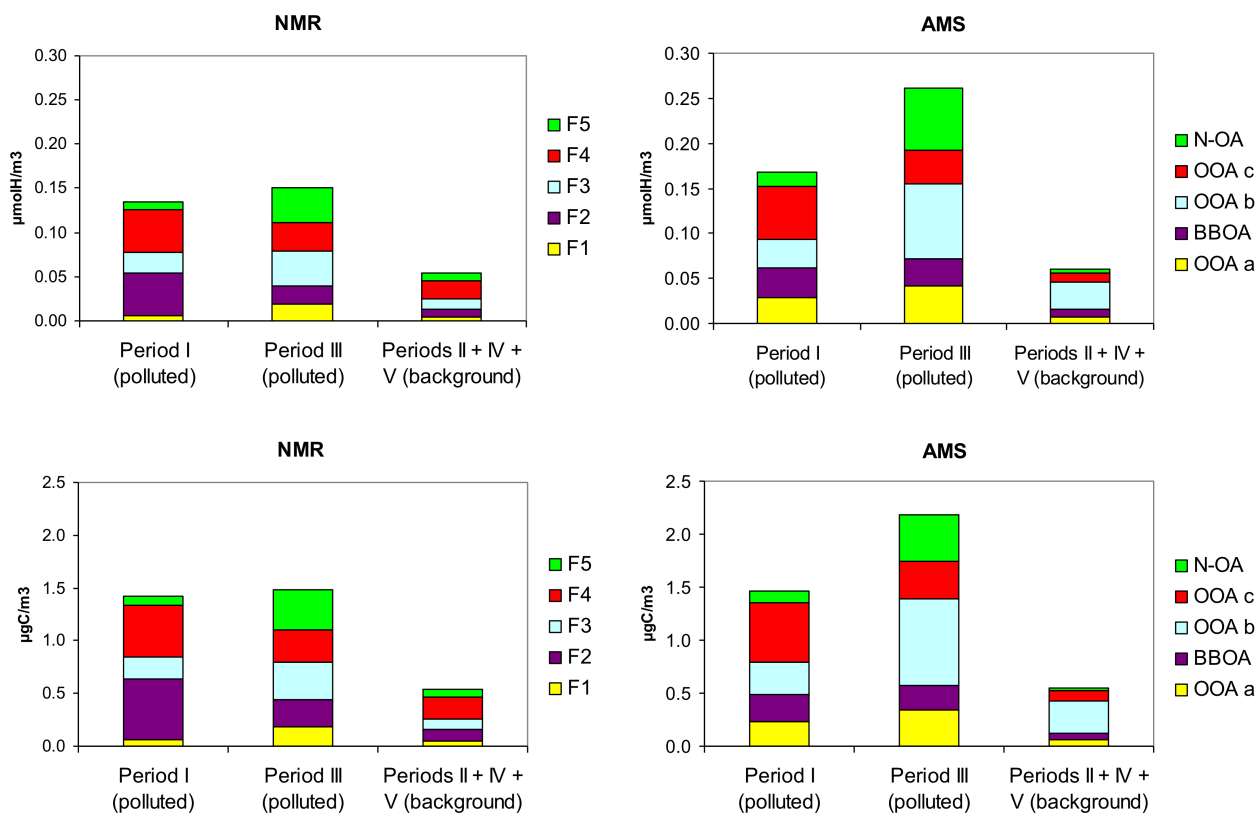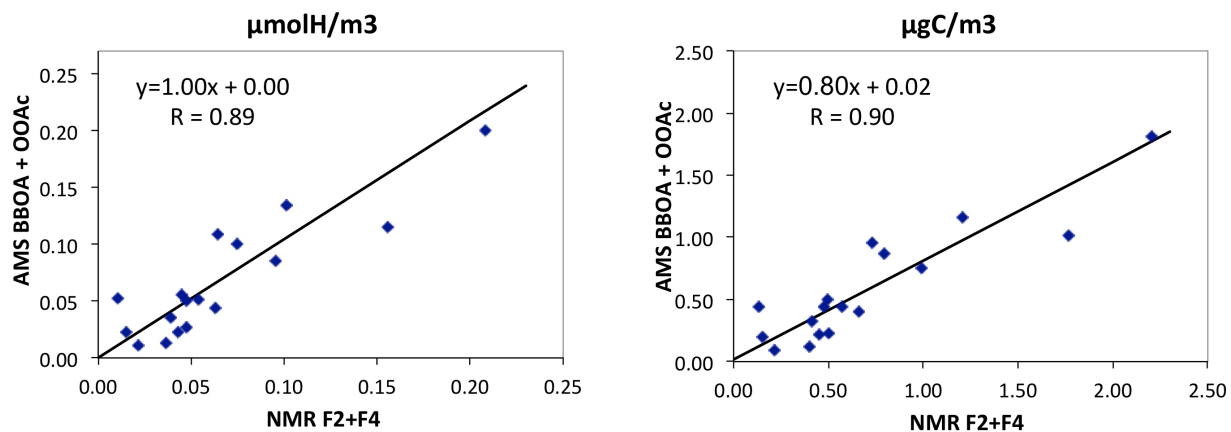
Fig. 6: Average concentrations of NMR and AMS factors for WSOC and OOA, respectively, in the three main periods of the field campaign. Concentrations are expressed in hydrogen (upper panels) and carbon units (lower panels).
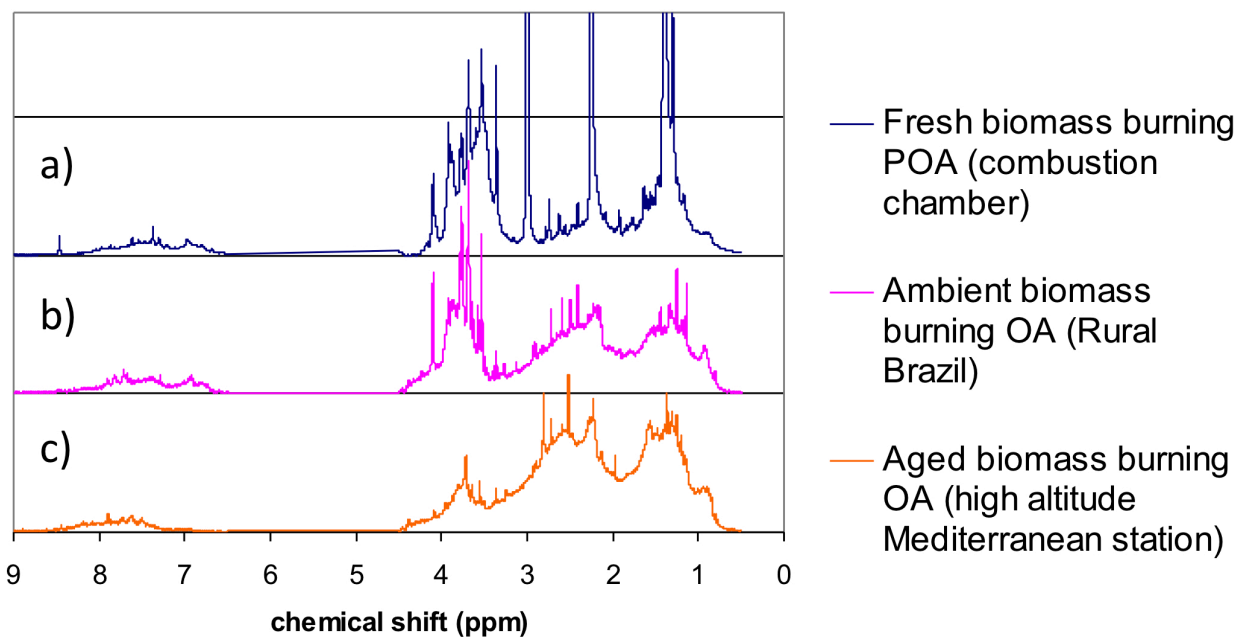

Fig. 7: Correlation plots between NMR and AMS total biomass burning contributions: NMR F2 + F4, and AMS BBOA + OOAc). An orthogonal fitting was used for the regression lines.

Fig. 8: Reference ^{1}H-NMR spectra for different stages of biomass burning aerosol ageing: a) laboratory wood burning POA (sharp peaks at 1.3, 2.2 and 3.3 ppm are from contaminants); b) ambient near-source biomass burning aerosol; c) biomass burning aerosol from long-range transport.
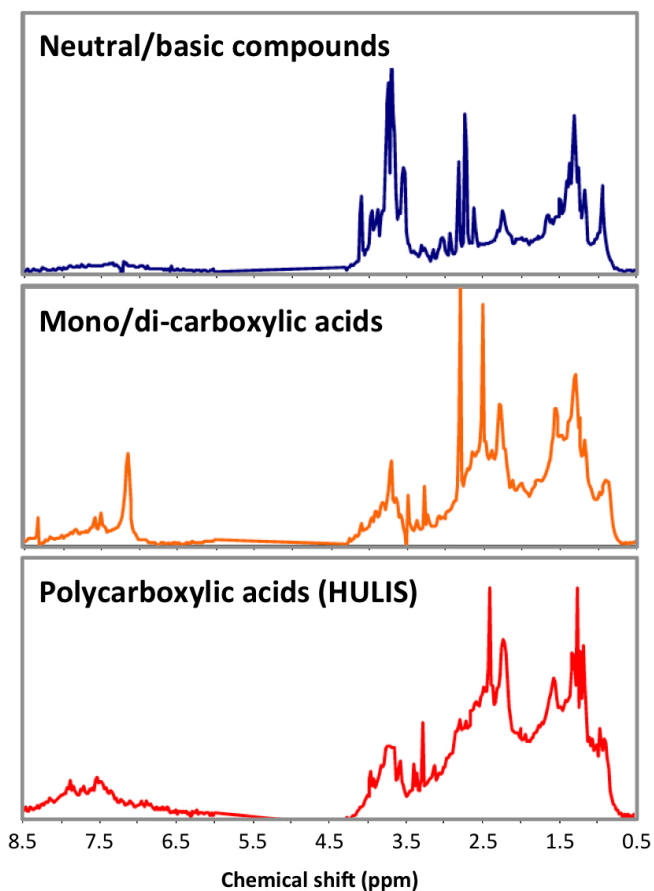
Fig. 9: ^{1}H-NMR spectra of WSOC fractions isolated by anion-exchange chromatography.

Whole campaign

8-20 April (Periods III, IV & V)
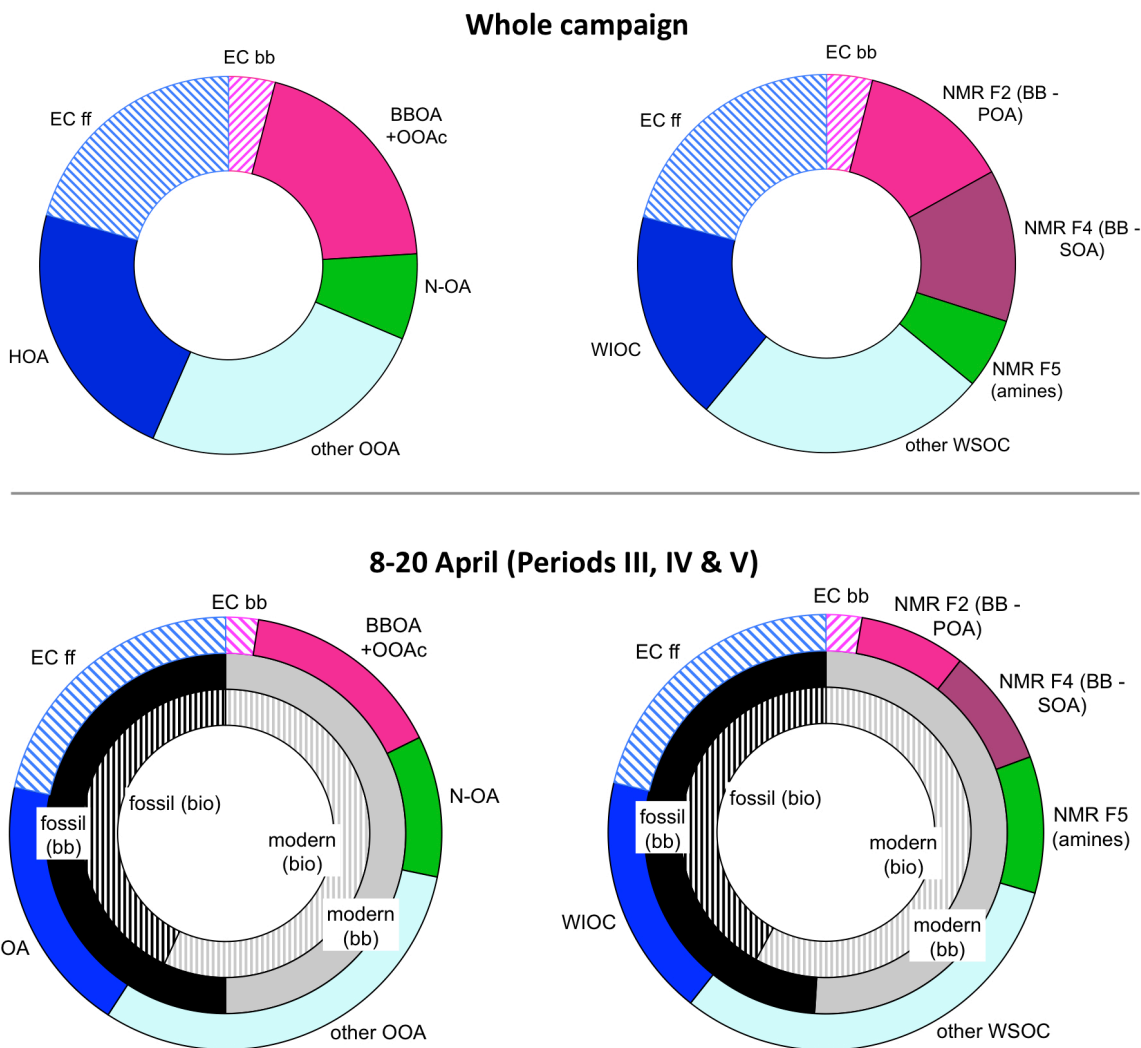
1236

1237 **Fig. 10**: Carbon budget of aerosol TC for the whole campaign (upper two panels) and for the period covered by the

1238 isotopic analyses (lower panels). Budgets are reconstructed based on PMF-AMS components (left) and NMR factors for

1239 WSOC (right). For more explanations refer to the text.

1240